

Article

Acoustic-Based Prediction of End-Product-Based Fibre Determinates within Standing Jack Pine Trees

Peter F. Newton

Canadian Wood Fibre Centre, Canadian Forest Service, Natural Resources Canada, Sault Ste. Marie, ON P6A 2E5, Canada; peter.newton@canada.ca; Tel.: +1-705-541-5615

Received: 6 June 2019; Accepted: 18 July 2019; Published: 23 July 2019



Abstract: The objective of this study was to specify, parameterize, and evaluate an acoustic-based inferential framework for estimating commercially-relevant wood attributes within standing jack pine (*Pinus banksiana* Lamb) trees. The analytical framework consisted of a suite of models for predicting the dynamic modulus of elasticity (m_e), microfibril angle (m_a), oven-dried wood density (w_d), tracheid wall thickness (w_t), radial and tangential tracheid diameters (d_r and d_t , respectively), fibre coarseness (c_o), and specific surface area (s_a), from dilatational stress wave velocity (v_d). Data acquisition consisted of (1) in-forest collection of acoustic velocity measurements on 61 sample trees situated within 10 variable-sized plots that were established in four mature jack pine stands situated in boreal Canada followed by the removal of breast-height cross-sectional disk samples, and (2) given (1), in-laboratory extraction of radial-based transverse xylem samples from the 61 disks and subsequent attribute determination via Silvscan-3. Statistically, attribute-specific acoustic prediction models were specified, parameterized, and, subsequently, evaluated on their goodness-of-fit, lack-of-fit, and predictive ability. The results indicated that significant ($p \leq 0.05$) and unbiased relationships could be established for all attributes but d_t . The models explained 71%, 66%, 61%, 42%, 30%, 19%, and 13% of the variation in m_e , w_t , s_a , c_o , w_d , m_a , and d_r , respectively. Simulated model performance when deploying an acoustic-based wood density estimate indicated that the expected magnitude of the error arising from predicting d_t , c_o , s_a , w_t , m_e , and m_a prediction would be in the order of $\pm 8\%$, $\pm 12\%$, $\pm 12\%$, $\pm 13\%$, $\pm 20\%$, and $\pm 39\%$ of their true values, respectively. Assessment of the utility of predicting the prerequisite w_d estimate using micro-drill resistance measures revealed that the amplitude-based w_d estimate was inconsequentially more precise than that obtained from v_d ($\approx <2\%$). A discourse regarding the potential utility and limitations of the acoustic-based computational suite for forecasting jack pine end-product potential was also articulated.

Keywords: wood quality; dilatational stress wave velocity; absolute and relative error intervals; Resistograph

1. Introduction

Global competition and societal change are eliciting incremental changes within the Canadian forest sector (sensu [1]). Forest management objectives and associated inputs are increasingly focused on enhancing end-product quality and value [2] and providing a wider array of ecosystem services (e.g., provisionary, regulatory, and cultural services [3]) while maintaining or increasing volumetric fibre yields. Realizing this aspirational trivariate goal will be partially dependent on the provision of enhanced operational intelligence and associated decision-making capacities in relation to the management and optimization of end-product flows within the upstream portion of the forest products supply chain.

The ability to forecast end-product potential of standing trees and (or) extracted logs is an important prerequisite for optimal in-forest value-based management decision-making. Operationally,

however, a priori knowledge of the internal fibre attributes, which are among the principal determinates underlying end-product quality (sensu [4]), are not readily observable or measurable within standing trees prior to harvest nor within the derived logs following harvest. Furthermore, forecasting end-product potential based on correlative relationships between external morphological tree characteristics and internal fibre attributes have yielded mixed results of generally limited utility [5]. Thus, apart from the implementation of a logistically-challenging destructive-based field sampling initiative combined with the subsequent expensive and time-consuming laboratory processing of extracted wood samples, end-product potential remains largely unknown at the time when critical in-forest allocation, segregation, and merchandizing decisions are being rendered. Consequently, opportunities to (1) identify high value stands during forest inventory assessments, (2) prioritize stand-level harvesting decisions according to end-product potential, (3) align harvesting decisions with real-time market demands, and/or (4) optimally manage wood flows based on the availability and capacity of conversion centres after harvest, are largely negated. These inability result in non-optimal decision-making throughout the upstream portion of the forest products supply chain, which results in overall reductions in economic efficiency.

Innovations in the development of non-destructive approaches that enable the indirect estimation of internal wood quality attributes, however, has yielded a suite of alternative methodologies and associated analytical platforms for forecasting end-product potential for both standing trees and harvested logs (sensu [6]). Acoustic-based estimation of internal attributes represents one of the more mature and operationally deployable non-destructive approaches, developed to date [5,7]. For example, forest practitioners currently have access to an array of acoustic-based tools that can provide an indirect measure of wood stiffness for (1) standing trees prior to harvest (e.g., Director ST300™ (Fibre-gen Inc., Christchurch, New Zealand) and TreeSonic™ microsecond timer (FAKOPP, Agfalva Hungary)), and (2) extracted logs following harvest (e.g., Hitman ST200 (Fibre-gen Inc.) and the Resonance Log Grader (FAKOPP)).

The acoustic approach to attribute estimation when applied to standing trees is based on the concept that the dynamic modulus of elasticity (MOE_{dyn} denoted as m_e in this study, GPa) of the xylem tissue encased within the main stem of softwood tree species, can in principle, be predicted from density-weighted acoustic velocity measurements [8–10]. More specifically, the velocity of a dilatational stress wave (hereafter, generically referred to as acoustic velocity and denoted as v_d (km/s)) arising from a mechanically-induced impact that propagates between a set of circumferential positioned probes, which traverses breast-height, is functionally related to the m_e , according to Equation (1) (sensu [11–13]).

$$m_e = f(P, w_{d(f)} v_d^2) \quad (1)$$

where P is the species or the sample-specific Poisson ratio (transverse to axial strain ratio) that is commonly treated as an unknown constant when parameterizing the relationship, and $w_{d(f)}$ is the species or sample-specific green wood density (kg/m^3) estimate. Statistically, acoustic-based attribute prediction models have frequently employed a simple linear model specification in which Silviscan-derived m_e estimates are expressed as a function of oven-dried wood density (w_d) and acoustic velocity (e.g., Equation (2)).

$$m_e = \beta_0 + \beta_1 w_d v_d^2 + \varepsilon \quad (2)$$

where β_0 and β_1 are species-specific intercept and slope parameters commonly estimated via ordinary least squares (OLS) regression analyses, and ε is a random error term. Previous research on standing red pine (*Pinus resinosa* Ait.) trees, which has utilized this modelling approach has revealed a satisfactory level of performance in terms of statistical significance, explanatory power, unbiasedness, and predictive ability [14]. Experimental results from other forest regions have also been supportive of this modelling approach. Hong [15] in a Swedish-based study reported a significant ($p \leq 0.05$) relationship that explained 59% of the variability in m_e within Scots Pine (*Pinus sylvestris* L.) trees.

The modulus of elasticity is a measure of wood stiffness, which reflects the degree of lateral displacement dimension lumber incurs when experiencing an extreme loading force: i.e., quantifies the degree of elasticity as measured by the amount of recoverable deformation (lateral displacement) that arises from increasing axial-based compression loads. Operationally, threshold ranges of the static variant of the modulus of elasticity along with physical dimensions, maximum knot size, and degree of warpage, are commonly used to stratify lumber products into various grade classes [16,17]. Although the static modulus of elasticity value for a given sample of wood is slightly lower in magnitude than its dynamic counterpart, their correlative interrelationship [18] enables the latter to be used extensively as a surrogate measure for reflecting the end-product potential [5]. More simplicity, but nevertheless based on the conceptual relationship underlying the acoustic approach as mathematically described by Equation (1), velocity measurements by themselves have been employed as wood quality response metrics in various fertilization [19], tree improvement [20], thinning [21], and management intensity [22] experiments.

Globally, the advent of the acoustic-based approach represents an innovative advancement in non-destructive wood quality detection methodologies, which has been shown to have considerable utility across a wide spectrum of forest management and research activities, as exemplified by numerous individual case assessments [23] and as documented in comprehensive literature reviews [24]. Overall, the traditional acoustic analytical framework, which has largely deployed the dynamic modulus of elasticity to forecast the solid wood end-product potential of standing trees and harvested logs, has been shown to be of consequential importance for informing segregation, allocation, and merchandizing decision-making [8]. However, most softwood species produce a wide array of end-products that are not always solely dependent on wood stiffness measures (*sensu* [25]). For example, secondary attributes such as microfibril angle, wood density, tracheid wall thickness, radial and tangential tracheid diameters, fibre coarseness, and specific surface area, are also important determinates of end-product potential [4].

Fortunately, acoustic-based estimation of these secondary attributes based on their correlative relationship with m_e has been shown to be viable for some softwood species. More particularly, as exemplified in the results reported for black spruce (*Picea mariana* (Mill.) B.S.P.), red pine and jack pine (*Pinus banksiana* Lamb.) and other species [14,26–32], among attribute correlative relationships, have been used to formulate a more encompassing acoustic-based inferential framework. Specifically, deploying the bivariate relationships between m_e and microfibril angle (MFA denoted m_a in this study, °), tracheid wall thickness (w_t , µm), radial and tangential tracheid diameters (d_r (µm) and d_t (µm), respectively), fibre coarseness (c_o , µg/m) and specific surface area (s_a , m²/kg), yielded the following suite of empirical-based secondary relationships applicable to standing softwood trees (*sensu* [14]): (1) $m_a \propto 1/m_e \Rightarrow m_a \propto (w_d v_d^2)^{-1}$; (2) $w_t \propto m_e \Rightarrow w_t \propto w_d v_d^2$; (3) $d_{r,t} \propto 1/m_e \Rightarrow d_{r,t} \propto (w_d v_d^2)^{-1}$; (4) $c_o \propto m_e \Rightarrow c_o \propto w_d v_d^2$; and (5) $s_a \propto 1/m_e \Rightarrow s_a \propto (w_d v_d^2)^{-1}$. Given that wood density is also among the principal attributes influencing end-product potential, its relationship with acoustic velocity has also been included within these frameworks ($w_d \propto v_d^2$). Actual empirical results arising from an evaluation of these secondary relationships for 54 standing red pine trees, revealed statistically viable relationships for five of the eight attributes examined (m_e , w_d , w_t , c_o , and s_a , [14]).

In order to further assess the generality of this expanded acoustic-based inferential framework for boreal conifers and potentially provide the prerequisite quantitative relationships that could improve in-forest segregation and allocation decision-making for other intensively-managed conifers, the primary objective of this study was to investigate, quantify, and evaluate this proposed suite of acoustic-based attribute relationships for standing jack pine trees. Furthermore, the potential deployment of this acoustic-based inferential framework is dependent on the provision of a wood density estimate. Promising results were attained previously for red pine trees where it was shown that wood density estimates could be derived either directly from acoustic velocity measurements or indirectly through the relationship between wood density and amplitude measures derived from resistance profiles generated from the Resistograph micro-drill tool (IML, Inc., Moultonborough, NH,

USA) [14,33]. However, the utility of these approaches for other boreal conifers is largely unknown. Thus, a secondary objective of this study was to examine the applicability of these approaches with regard to estimating w_d for standing jack pine trees.

2. Materials and Methods

2.1. Study Sites, Sample Tree Selection, Acoustic Velocity Measurements, and Destructive Stem Analysis Procedures

Sixty-one trees from two geographically-separated (450 km) long-term (monitored for 20+ years) jack pine thinning experiments located in the north-eastern (denoted the Sewell site, which falls within the Sewell River watershed area) and north-central (denoted the Tyrol site, which falls within the western portion of the Namewaminkan River watershed area) regions of the Canadian province of Ontario, were selected for analyses. The trees were grown under a nominal range of silvicultural intensities that are reflective of the forest management strategies currently employed in the central portion of the Canadian Boreal Forest Region [34]. Specifically, allowing natural regeneration to restock recently disturbed sites followed by the implementation of one of three crop planning regimes: (1) extensive regime in which no density management treatments were implemented, (2) low intensity regime involving the early application of precommercial thinning (PCT) treatments so that the time for operability status could be reduced, and (3) a high intensity regime involving PCT and commercial thinning (CT) treatments in order to capture merchantable volume mortality losses diversify end-product potential at rotation.

At the Sewell site, 31 jack pine sample trees were selected within six variable-size plots that were established in three jack pine stands that regenerated naturally following a stand-replacing wildfire event during the 1958–1960 period. The stands were situated on medium-to-good quality sites (mean site index of 18 m@50 yr, [35]), geographically located within Forest Section B.7—Missinaibi-Cabonga of the Canadian Boreal Forest Region [36], and were approximately 53 years of age at breast height (1.3 m) when sampled. The glacial-derived soils were characterized as deep (>1 m) with coarse-to-medium sandy textures situated on gently undulating (rolling) topography. Silviculturally, the stands were subjected to one of three treatments, which resulted in three different density management regimes: (1) un-thinned controls, (2) PCT at age 11 (1971), and (3) PCT at age 11 followed by a light pseudo-CT at age 43 (2003).

At the Tyrol site, 30 jack pine sample trees were selected within four variable-size plots that were established in two jack pine stands that regenerated naturally following a stand-replacing wildfire event during the early 1940s. The stands were situated on good-to-excellent quality sites (mean site index of 21 m@50 year, [35]), geographically located within Forest Section B9 (Superior) of the Canadian Boreal Forest Region [36], and were approximately 73 years of age at breast height when sampled in 2015. Similar to the Sewell site, the soils were characterized as deep (>1 m) with fine sandy textures situated on gently rolling topography. These stands were subjected to two density manipulation treatments: PCT at age 20 (1962) followed a light pseudo-CT treatment during 1998 at the age of approximately 56.

At the conclusion of the 2013 and 2015 vegetative growing seasons at the Sewell and Tyrol sites, respectively, the diameter at breast-height (1.3 m) outside-bark diameter, total height, height-to-live crown, and acoustic velocity measurements were obtained from each sample tree before they were felled and sectioned, which deployed destructive stem analysis techniques. Specifically, the v_d (km/s) propagating throughout each standing tree between probes inserted to an appropriate depth of 2 cm into the xylem tissue (wood-inside bark) at stem heights of 0.3 m and 1.5 m, was measured using the Director ST300 time-of-flight acoustic velocity tool (Fibre-gen Inc., Christchurch, New Zealand (www.fibre-gen.com)). A twice-replicated measurement set consisting of eight sequential measurements on each of the north, east, south, and west cardinal-based circumferential surfaces was obtained. These cardinal-based mean v_d values were then used to generate a composite grand mean value for each tree. Additionally, probe distances, ambient air temperatures, and bark surface temperatures were recorded at the time of each acoustic velocity measurement, and the Director ST300 was validated in terms of

measurement accuracy thresholds as per manufacture specifications before the field data acquisition activities commenced.

Following the attainment of the standing tree measurements, each sample tree was felled at stump height (≈ 0.3 m), delimbed, and the stem topped at an 80% relative height position. The stem was then sectioned into 0%–20%, 20%–40%, 40%–60%, and 60%–80% log-length intervals employing a percent height stem analysis sampling protocol. Cross-sectional samples were extracted at stump height, breast-height (1.3 m), relative height positions of 10%, 30%, 50%, and 70% (centre-point of each of the four logs), and at the 80% relative height position, which yielded a total of seven disks per tree. These disks were immediately (≤ 8 h) placed in cold storage (< 0 °C) and then transported to and placed in long-term cold storage facilities until laboratory processing commenced. The 61 breast-height cross-sectional disks comprised the data set used to parameterize the primary and secondary attribute—acoustic velocity relationships, examined in this study. Table 1 provides a descriptive statistical summary of the mensurational characteristics and acoustic velocity measurements of the selected sample trees. The remaining log-based disks were used to examine longitudinal stress wave velocity-attribute relationships, as reported in a concurrent study by Newton [27]. The breast-height disks along with the corresponding 61 stump disks were also used to assess the Resistograph-based amplitude—wood density relationship. In order to partially illustrate these data acquisition procedures, a pictorial exemplification is given in Figure 1.

2.2. Silviscan-Based Attribute Determination and Related Computations

In the laboratory, a geometric mean diameter on each disk, which was devoid of intersections with radial checks or embedded knots if present, was demarked (see Figure 1). A transverse 2×2 cm bark-to-pith-to-bark sample was then extracted along the demarked diameter from which a pith-to-bark radial sequence was randomly selected for Silviscan-3 analysis (see Figure 1). These sequences were then subjected to extraction techniques so that resins, which could influence density estimates, were removed prior to attribute determination. The analyses consisted of soaking the samples in acetone for 12 h, which was followed by extraction for 8 h at 70 °C using a modified Soxhlet system. The sequences were then air-dried for approximately 12 h, conditioned to a 40% relative humidity at a temperature of 20 °C, and then processed and subsequently subjected to fibre determination employing the SilviScan-3 system. The system provided area-weighted mean annual ring estimates of (1) radial and tangential tracheid diameters and tracheid wall thickness as directly determined via image analysis [37], (2) wood density as directly derived from X-ray densitometry [37], (3) microfibril angle as directly ascertained through X-ray diffraction [38], (4) modulus of elasticity as indirectly determined via a combination of X-ray densitometry and diffraction measurements [39], and (5) fibre coarseness and specific surface area as indirectly determined using cell dimensions and wood density estimates [37].

Computationally, the resultant annual ring estimates for m_e , w_d , m_a , w_t , d_r , d_t , c_o , and s_a were used to compute attribute-specific cumulative area-weighted moving average values for each radial sequence (Equation (3)).

$$F_{(k)} = \sum_{j=1}^n f_{(k)j} a_j / \sum_{j=1}^n a_j \quad (3)$$

where $F_{(k)}$ is the cumulative moving area-weighted average value for the k th attribute, which is calculated in the pith-to-bark direction and terminates at the outermost ring, $f_{(k)j}$ is the value of the k th attribute for the j th annual ring, and a_j is the area of the j th annual ring (mm^2). Table 2 includes a descriptive statistical summary of the fibre attributes measured.

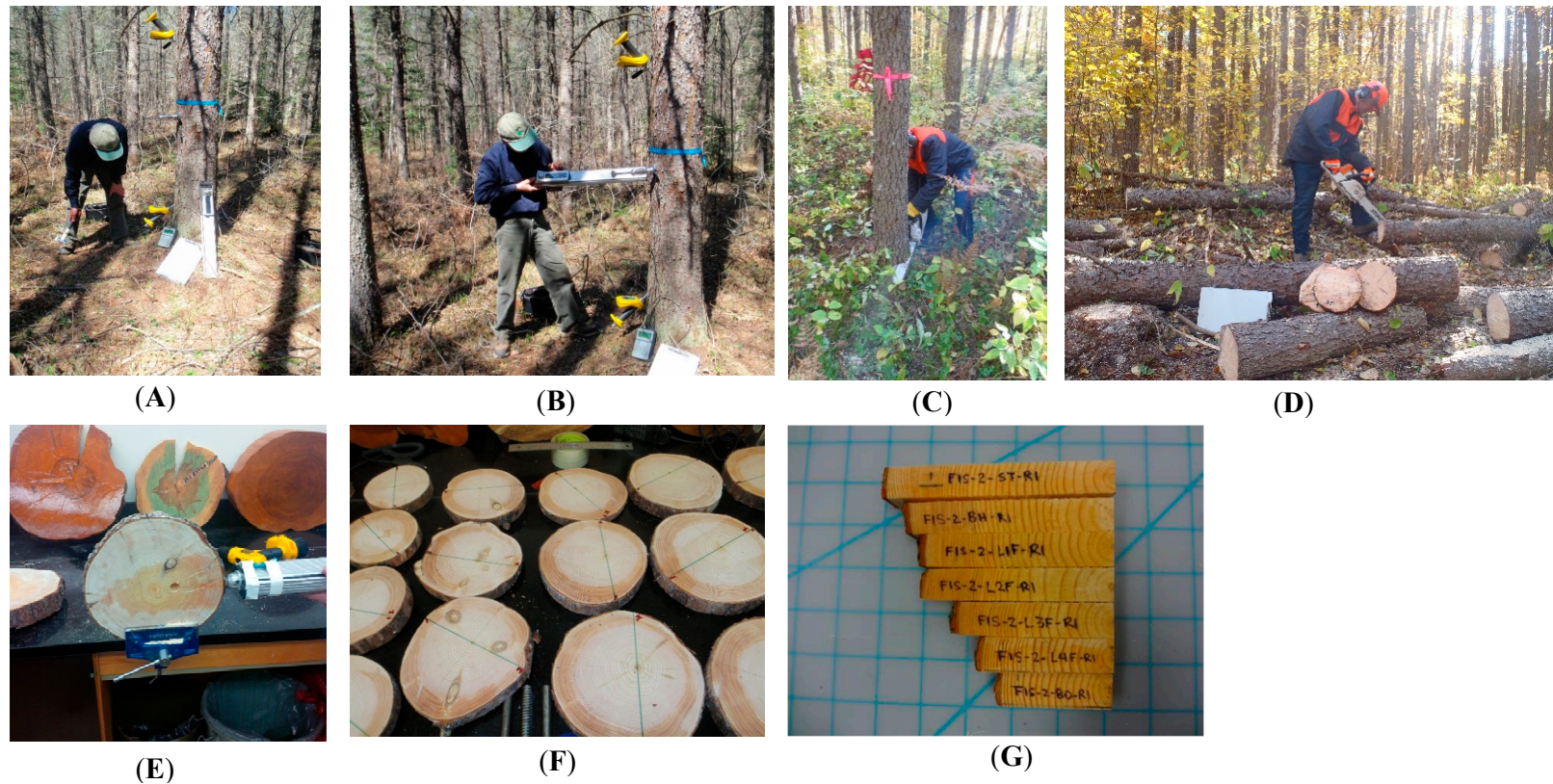


Figure 1. Sequential pictorial exemplification of in-forest and in-lab data acquisition procedures preceding wood attribute determination via Silviscan-3 and subsequent statistical analytics: (A) acoustic sampling of standing jack pine tree with Director ST-300 time-of-flight instrument with yellow probes and hammer impact action shown (i.e., generating and measuring the dilatational stress wave). (B) Resistograph micro-drill sampling at breast-height, (C) felling a sample tree, (D) destructive stem analysis on a delimited and topped tree and extraction of cross-sectional disk samples, (E) in-lab extraction of resistance profiles via the Resistograph (e.g., from bark to artificially created circular-shaped void). (F) Demarcation of the geometric mean diameter on each cross-sectional disk, and (G) extracted and random selected 2 × 2 cm pith-to-bark radial sequences from one sample tree (e.g., seven labelled sequences extracted from the stump height (-ST-) and breast-height (-BH-) cross-sectional disks, and those at relative heights of 10% (-L1F-), 30% (-L2F-), 50% (-L3F-), 70% (-L4F-), and 80% (-80-)).

Table 1. Descriptive statistical summary of the mensurational characteristics and acoustic velocity measurements of the 61 sample trees by site ($n = 31$ and 30 for Sewell and Tyrol, respectively).

Variable	Site	Mean	Standard Deviation	Minimum	Maximum	CV ^a (%)
Diameter at breast-height (cm)	Sewell	18.8	2.11	14.7	22.6	11.2
	Tyrol	24.4	2.17	19.8	29.1	8.9
	Combined	21.5	3.54	14.7	29.1	16.5
Breast-height age (year)	Sewell	50.2	0.96	47	51	1.9
	Tyrol	68.7	1.27	66	71	1.9
	Combined	59.3	9.36	47	71	15.8
Total height (m)	Sewell	21.1	1.26	18.3	22.9	6.0
	Tyrol	22.2	1.57	19.5	24.6	7.1
	Combined	21.7	1.52	18.3	24.6	7.0
Live crown ratio (%)	Sewell	26.1	4.50	15.0	35.3	17.3
	Tyrol	28.2	7.20	14.1	41.5	25.5
	Combined	27.1	6.04	14.1	41.5	22.3
Dilatational stress wave velocity (km/s)	Sewell	4.31	0.18	3.98	4.65	4.2
	Tyrol	4.59	0.16	4.26	4.92	3.4
	Combined	4.45	0.22	3.98	4.92	5.0
Bark temperature (°C)	Sewell	12.0	5.70	3.2	20.2	47.6
	Tyrol	16.5	6.09	4.8	25.1	36.9
	Combined	14.2	6.27	3.2	25.1	44.2

a: Coefficient of variation.

Table 2. Descriptive statistical summary of the cumulative area-weighted fibre attributes at breast-height of the 61 sample trees by site ($n = 31$ and $n = 30$ for Sewell and Tyrol, respectively).

Variable	Site	Mean	Standard Deviation	Minimum	Maximum	CV ^a (%)
Modulus of elasticity (m_e , GPa)	Sewell	11.48	1.61	8.25	15.21	14.0
	Tyrol	13.64	1.46	10.76	16.27	10.7
	Combined	12.54	1.87	8.25	16.27	14.9
Wood density (w_d , kg/m ³)	Sewell	422.7	27.66	358.1	480.9	6.5
	Tyrol	453.7	26.36	405.9	509.4	5.8
	Combined	437.9	31.04	358.1	509.4	7.1
Microfibril angle (m_a , °)	Sewell	14.31	3.19	8.09	20.69	22.3
	Tyrol	13.47	2.55	9.66	18.69	18.9
	Combined	13.90	2.90	8.09	20.69	20.9
Tracheid wall thickness (w_t , µm)	Sewell	2.66	0.18	2.24	3.06	6.8
	Tyrol	2.85	0.22	2.46	3.27	7.6
	Combined	2.75	0.22	2.24	3.27	8.0
Tracheid radial diameter (d_r , µm)	Sewell	31.1	1.32	28.4	33.5	4.2
	Tyrol	30.5	1.02	28.3	33.2	3.4
	Combined	30.8	1.22	28.3	33.5	4.0
Tracheid tangential diameter (d_t , µm)	Sewell	27.8	0.77	26.6	29.7	2.8
	Tyrol	27.6	0.56	26.2	28.4	2.0
	Combined	27.7	0.68	26.2	29.7	2.5
Coarseness (c_o , µg/m)	Sewell	403.3	22.86	366.4	458.6	5.7
	Tyrol	421.2	30.03	368.0	481.9	7.1
	Combined	412.1	27.91	366.4	481.9	6.8
Specific surface area (s_n , m ² /kg)	Sewell	318.9	16.68	285.1	355.3	5.2
	Tyrol	298.3	18.76	263.9	338.2	6.3
	Combined	308.7	20.43	263.9	355.3	6.6

a: Coefficient of variation.

2.3. Resistograph-Based Micro-Drill Resistance Measurements and Associated Computations

In order to evaluate the relationship between mean amplitude and wood density using a larger sample set, the cross-sectional disks sampled at both breast-height and at stump height were deployed. Procedurally, this involved obtaining the semi-circular cross-sectional segments remaining after the bark-to-pith-to-bark transverse sample was extracted and subjected them to micro-drill resistance analysis using the PD400 Resistograph (IML, Inc., Moultonborough, NH, USA). First, on each semi-circular segment, the number of rings (years) proceeding from the (1) bark to the edge of the segment on the Sewell disks, or (2) bark to a manually created void on the Tyrol disks, was determined (see Figure 1). This ring count value was then used to derive the corresponding cumulative moving area-weighted wood density estimate for that specific partial disk sequence employing the Silviscan-3 data (denoted w'_d (kg/m^3)). Second, twice replicate micro-drill resistance profiles consisting of percent-based amplitude measurements were obtained at every 0.1 mm from each disk segment using a fixed 100 cm/min feed rate and a 2500 rpm rotational speed setting. These profiles were transferred to a PC and edited using the PD-Tools Pro software program (IML, Inc., Moultonborough, NH, USA). The editing step consisted of removing the amplitude measurements associated with the periderm and voids thus yielding only the profile measurements corresponding to the delineated partial sequence on each disk segment. The mean amplitude was then determined for each of the two drill profiles from which a segment-specific grand mean amplitude was calculated (denoted a_m (%)). In total, 122 w'_d - a_m observational pairs from the 61 sample trees were available for analysis. Table 3 provides a descriptive summary of these measurements.

Table 3. Descriptive statistical summary of the mean amplitude and corresponding wood density measurements derived from the 122 cross-sections found in the stump and breast-height disks from the two sites (two disks/tree \times 31 sample trees at Sewell (62) and two disks/tree \times 30 sample trees at Tyrol (60) yielded 122 observational pairs).

Variable	Site	Mean	Standard Deviation	Minimum	Maximum	CV ^a (%)
Mean amplitude (a_m ; %)	Sewell	15.80	2.72	9.90	21.30	17.2
	Tyrol	23.80	4.80	14.94	37.25	19.4
	Combined	20.19	5.92	9.90	37.25	29.3
Wood density (w'_d ; kg/m^3)	Sewell	429.0	30.92	358.3	511.0	7.2
	Tyrol	468.1	31.68	383.5	548.1	6.8
	Combined	448.2	36.09	358.3	548.1	8.2

a: Coefficient of variation.

2.4. Fibre Attribute—Acoustic Velocity and Amplitude Density Prediction Models

Graphical and correlation analyses were used during the initial model specification phase to determine candidate acoustic-based functional relationships for each attribute. Specifically, deploying the SilviScan-3-based oven-dried wood density (w_d ; kg/m^3) estimate as a surrogate measure for its fresh density counterpart, bivariate scatter plots, and associated correlation coefficients for the following relationships were examined: $m_e \propto w_d v_d^2$, $w_d \propto v_d^2$, $m_a \propto (w_d v_d^2)^{-1}$, $w_t \propto w_d v_d^2$, $d_r \propto (w_d v_d^2)^{-1}$, $d_t \propto (w_d v_d^2)^{-1}$, $c_o \propto w_d v_d^2$, and $s_a \propto (w_d v_d^2)^{-1}$. The resultant scatterplots which exhibited definable trends, were mostly linear in nature and, hence, supportive of the usage of the simple linear functional form. However, to ensure that non-linear patterns if present were detected, similarly structured bivariate scatterplots and derived correlation coefficients were also examined following log-linear, log-log, inverse, and non-linear power-based transformations. These transformations, however, did not increase the degree of linearity nor reveal the presence of nonlinearity, as subjectively determined from visual interpretations of the resultant bivariate scatterplots, and objectively determined from analyzing changes in the Pearson-moment correlation coefficients. Thus, the simple linear formulation as exemplified by the regression equation given by Equation (2) for m_e was provisionally accepted as

the specification to be used in quantifying all eight acoustic-attribute relationships. However, pending the full acceptance of this specification, the effect of site evaluated.

With regard to assessing the site effect, the relationship between each area-weighted cumulative moving average fibre attribute value and associated density-weighted or density-unweighted acoustic velocity value was quantified using a multiple regression model specification that included site-specific indicator variables for both the intercept and slope parameters (Equations (4a) and (4b)).

$$F' = \beta_0 + \beta'_0 i_v + \beta_1 w_d v_d^2 + \beta'_1 i_v w_d v_d^2 + \varepsilon \quad (4a)$$

$$w_d = \beta_0 + \beta'_0 i_v + \beta_1 v_d^2 + \beta'_1 i_v v_d^2 + \varepsilon \quad (4b)$$

where F' is the area-weighted cumulative value at the time of sampling for the k' th attribute ($k' = m_e, m_a, w_t, d_r, d_t, c_o,$ and s_a), i_v is an indicator variable denoting geographic site location (sample trees selected from the Sewell and Tyrol sites are numerically coded as zero and unity, respectively), $\beta_i, i = 0, 1$ and $\beta'_i, i = 0, 1$ are parameters specific to each attribute and site that are estimated via OLS regression analysis, and ε is a random error term specific to each attribute. These preliminary regressions were assessed for the presence of outliers and influential observations through subjective interpretation of the bivariate predictor variable—raw residual plots and objective assessment of residual statistical measures (i.e., studentized deleted residuals and Cook's distance where the probability level for exclusion was set at 0.01 [40]). If present, the suspect observational pair(s) was removed from the data set and the models were re-parameterized. The resultant parameter estimates for the indicator variables were then assessed for their significance at the 0.05 probability level. This preliminary assessment indicated that seven of the eight attribute relationships ($m_e, w_d, m_a, w_t, d_r, c_o,$ and s_a) deploying the simple linear model attained statistical significance ($p \leq 0.05$), and six of the seven relationships ($m_e, w_d, m_a, w_t, c_o,$ and s_a) revealed no evidence of the presence of a significant ($p \leq 0.05$) site effect. Consequently, in order to maintain a standardized model specification across all attributes, and, in light of the lack of a site effect for the majority (86%) of the relationships, the simple linear regression models as specified by Equations (5a) and (5b), were employed.

$$F' = \beta_0 + \beta_1 w_d v_d^2 + \varepsilon \quad (5a)$$

$$w_d = \beta_0 + \beta_1 v_d^2 + \varepsilon \quad (5b)$$

where β_0 and β_1 are attribute-specific intercept and slope parameters, respectively, estimated via OLS regression analysis, and ε is an attribute-specific random error term. With reference to the applicability of an alternative mixed-effects regression specification inclusive of random and fixed effects, a two-level hierarchical linear model specification was evaluated. This model consisted of simple linear formulations where the intercept parameter was treated as random (i.e., allowed to vary by tree) and the slope parameter was treated as fixed (sensu [26,27]). Following parameterization by deploying a hierarchical linear and nonlinear modeling software algorithm (HLM7, [41]), the statistical assessment of the resultant models indicated an absence of significant ($p \leq 0.05$) random effects across all eight attributes, and hence negated further consideration of the mixed-effects specification.

In order to select a specification for the relationship between w'_d and a_m , graphical and correlation analyses similar to that conducted for the attribute—acoustic velocity relationships were implemented. Resultantly, given the linear trend exhibited and the associated significance ($p \leq 0.05$) and magnitude (0.71) of the correlation coefficient attained, a simple linear regression specification was selected for parameterization (Equation (6)).

$$w'_d = \beta_0 + \beta_1 a_m + \varepsilon \quad (6)$$

where β_0 and β_1 are intercept and slope parameters, respectively, and ε is a random error term.

The statistical evaluation of all the regression relationships followed the same protocol employed previously for the red pine trees, as described by Newton [14]. Specifically, each regression relationship

was evaluated for their compliance with the constant variance and normality assumptions underlying OLS parameterization using residual statistics and graphical analysis including normal probability plots. Additionally, each regression relationship was assessed for the presence of potential outliers and influential observations, as determined using the predictor variable—raw residual graphs in association with residual statistics following the procedures previously described ([40]). If present, the suspect observational pair(s) was/were removed and the relationship re-parameterized. The relationships were then evaluated on their goodness-of-fit and lack-of-fit characteristics, and predictive ability: i.e., (1) explanatory power as measured by the proportion of variability explained (coefficient of determination) was employed as an overall goodness-of-fit measure, (2) absolute and relative mean biases (Equations (7) and (8), respectively) and their 95% confidence intervals (Equation (9)) were used to evaluate the presence of systematic lack-of-fits, and (3) predictive precision as measured by the employment of 95% prediction and tolerance error intervals were used to assess the predictive ability (Equations (10) and (11), respectively [42,43]).

$$\bar{B}_{a(k)} = \sum_{i=1}^{n(k)} (V_{(i)(k)} - \hat{V}_{(i)(k)}) / n(k) \quad (7)$$

$$\bar{B}_{r(k)} = \sum_{i=1}^{n(k)} \left(100 \frac{(V_{(i)(k)} - \hat{V}_{(i)(k)})}{V_{(i)(k)}} \right) / n(k) \quad (8)$$

$$\bar{B}_{a,r(k)} \pm \frac{S_{a,r(k)} \cdot t_{(n(k)-1,0.975)}}{\sqrt{n(k)}} \quad (9)$$

$$\bar{B}_{a,r(k)} \pm \sqrt{1/n(k) + 1/n_p} \cdot S_{a,r(k)} \cdot t_{(n(k)-1,0.975)} \quad (10)$$

$$\bar{B}_{a,r(k)} \pm g(\lambda, n(k), P) \cdot S_{a,r(k)} \quad (11)$$

where $\bar{B}_{a(k)}$ and $\bar{B}_{r(k)}$ are the mean absolute and relative error specific to the k th attribute, respectively, $V_{(i)(k)}$ and $\hat{V}_{(i)(k)}$ are the observed and predicted value of the k th attribute for the i th sample tree, $n(k)$ is the number of predicted-observed pairs specific to the k th attribute, $S_{a,r(k)}$ is the standard deviation of the absolute ($S_{a(k)}$) or relative ($S_{r(k)}$) biases specific to the k th attribute, $t_{(n(k)-1,0.975)}$ is the 0.975 quantile of the t -distribution with $n(k)-1$ degrees of freedom specific to the k th attribute, n_p is the number of future predictions considered (e.g., a single newly sampled tree ($n_p = 1$) or a group of newly sampled trees within a given stand ($n_p = 30$)), and g is a normal distribution tolerance factor specifying the probability (λ) that, at least a proportion of the distribution of errors (p ; 95%), will be included within the stated tolerance interval.

The magnitude of error expected when using an acoustic-based wood density estimate as input to the density-weighted attribute prediction equations, was also assessed. Computationally, this involved employing the acoustic velocity measurement for each sample tree in conjunction with the parameterized wood density prediction equation in order to generate a density estimate. Inputting the density estimate along with the acoustic velocity measurement into the parameterized attribute-specific equations yielded a suite of attribute estimates for each tree. This suite of estimates along with the corresponding observed values were then used to calculate (1) lack-of-fit and prediction error metrics in both absolute and relative terms (mean biases (sensu Equations (7) and (8)) and associated 95% confidence intervals (sensu Equation (9)), and (2) prediction and tolerance error intervals (sensu Equations (10) and (11), respectively, [42,43]).

3. Results

3.1. Fibre Attribute—Acoustic Velocity Models for Standing Jack Pine Trees

Based on the acoustic velocity measurements, which ranged from 3.89 to 4.92 km/s and Silviscan-3 wood attribute estimates obtained from the 61 standing jack pine sample trees, viable regression relationships were obtained for seven of the eight attributes considered (see Table 1; Table 2 for a

complete set of the descriptive statistics of the measurements and attribute estimates). Specifically, the parameter estimates and associated regression statistics for the wood density weighted and unweighted relationships (Equations (5a) and (5b)) are given in Table 4 and graphically illustrated in Figure 2. As tabulated and shown, the relationships were significant ($p \leq 0.05$) for the following seven relationships: m_e , m_a , w_t , d_r , c_o , and $s_a = f(\beta_{0,1}, w_d v_d^2)$ and $w_d = f(\beta_{0,1}, v_d^2)$. In terms of goodness-of-fit, the proportion of variability in the attribute-specific dependent variable explained by the significant ($p \leq 0.05$) regressions ranged from a relatively low value of 0.13 to a moderately high value of 0.71, as measured by the coefficient of determination (r^2 , Table 4). Among attribute comparisons based on the percentage of variability explained, yielded the following highest-to-lowest ordered ranking: 71% for $m_e - w_d v_d^2 > 66\%$ for $w_t - w_d v_d^2 > 61\%$ for $s_a - w_d v_d^2 > 42\%$ for $c_o - w_d v_d^2 > 30\%$ for $w_d - v_d^2 > 19\%$ for $m_a - w_d v_d^2 > 13\%$ $d_r - w_d v_d^2$. Assessment of the multitude and significance of the biasedness exhibited by each relationship indicated that the parameterized models were unbiased (Table 5). The mean absolute and relative biases were not significantly ($p \leq 0.05$) different from zero, as inferred from the 95% confidence intervals. Examining the attribute—acoustic velocity observational pairs for each relationship qualitatively confirmed the absence of consequential lack-of-fits among the fitted models.

Table 4. Parameter estimates and statistics for the attribute—acoustic velocity regression relationships (Equations (5a) and (5b)).

Relationship	Parameter Estimates ^a		df	Regression Statistics ^b		
	Intercept	Slope		r^2	SEE	F-Ratio
	(n_{reg}, n_{res})					
$m_e - w_d v_d^2$	1.934392	0.001217	1, 59	0.710	1.018	144.6 *
$w_d - v_d^2$	267.449930	8.598452	1, 59	0.299	26.212	25.1 *
$m_a - w_d v_d^2$	22.358915	-0.000971	1, 59	0.189	2.635	13.7 *
$w_t - w_d v_d^2$	1.587713	0.000133	1, 58	0.662	0.125	113.4 *
$d_r - w_d v_d^2$	33.728448	-0.000336	1, 59	0.127	1.152	8.6 *
$d_t - w_d v_d^2$	28.437516	-0.000091	1, 58	0.034	0.625	2.1 ^{ns}
$c_o - w_d v_d^2$	295.366197	0.013288	1, 58	0.422	20.399	42.4 *
$s_a - w_d v_d^2$	416.120177	-0.012317	1, 59	0.613	12.819	93.4 *

a: OLS parameter estimates for the intercept (β_0) and slope (β_1) (Equations (5a) and (5b)). b: Degrees of freedom (df) for regression (n_{reg}) and residual error (n_{res}), coefficient of determination (r^2), and standard error of the estimate (SEE where units are specific to the dependent variable: GPa, kg/m³, °, μm, μm, μg/m, and m²/kg for m_e , w_d , m_a , w_t , d_r , d_t , c_o , and s_a , respectively), and F-statistic where superscripts * and ns denote a significant ($p \leq 0.05$) and non-significant ($p > 0.05$) relationship, respectively.

Table 5. Lack-of-fit and predictive ability of the significant ($p \leq 0.05$) density-weighted and density-unweighted acoustic velocity-attribute relationships (Equations (5a) and (5b)).

Relationship	Lack-of-Fit Measures ^a				Predictive Ability: 95% Error Intervals ^c			
	Absolute ^b		Relative (%)		Prediction		Tolerance	
	Mean bias	95% CL	Mean bias	95% CL	Absolute ^b 95% CL	Relative (%) 95% CL	Absolute ^b 95% CL	Relative (%) 95% CL
$m_e - w_d v_d^2$	0.000	±0.259	0.715	±2.259	±2.035	<u>±17.8</u>	±2.350	<u>±20.5</u>
$w_d - v_d^2$	0.000	±6.659	0.351	±1.527	±52.429	±12.0	±60.535	±13.9
$m_a - w_d v_d^2$	0.000	±0.669	3.607	±5.214	±5.270	<u>±41.1</u>	±6.085	<u>±47.4</u>
$w_t - w_d v_d^2$	0.000	±0.032	0.203	±1.183	±0.250	±9.2	±0.289	±10.7
$d_r - w_d v_d^2$	0.000	±0.293	0.136	±0.960	±2.304	±7.6	±2.660	±8.7
$c_o - w_d v_d^2$	0.000	±5.226	0.240	±1.294	±40.816	±10.1	±47.182	±11.7
$s_a - w_d v_d^2$	0.000	±3.256	0.168	±1.062	±25.640	±8.4	±29.605	±9.7

a: Mean absolute (Equation (7)) and relative (Equation (8)) bias and the limits (CL) of the associated 95% confidence interval (Equation (9)) where mean values not significantly ($p > 0.05$) different from zero were indicative of an unbiased relationship. b: Absolute error units are attribute-specific: GPa, kg/m³, °, μm, μm, μg/m, and m²/kg for m_e , w_d , m_a , w_t , d_r , c_o , and s_a , respectively. c: Confidence limits (CL) for the 95% prediction and tolerance error intervals for absolute and relative errors (Equations (10) and (11), respectively): mean bias ± 95% CL. Specifically, there is a 95% probability that a future error will be within the stated prediction interval and that there is a 95% probability that 95% of all future errors will be within the stated tolerance interval [42,43]. Underlined values denote approximate values given non-normality of the error distributions at the 0.05 probability level.

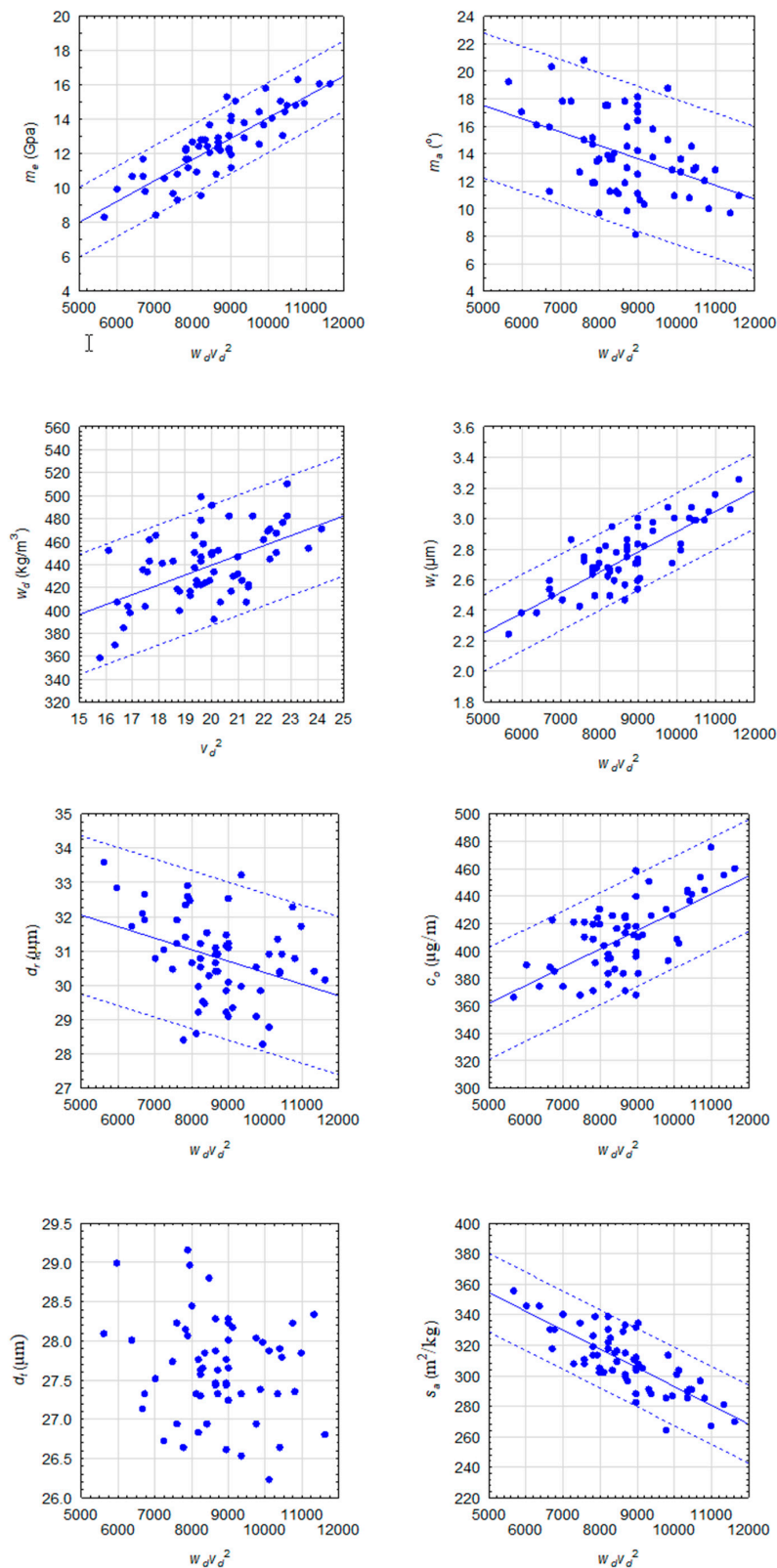


Figure 2. Attribute-specific acoustic relationships with significant ($p \leq 0.05$) regression relationships superimposed (solid line, Equations (5a) and (5b), Table 4) for dynamic modulus of elasticity ($m_e = f(w_d v_d^2)$), wood density ($w_d = f(v_d^2)$), microfibril angle ($m_a = f(w_d v_d^2)$), tracheid wall thickness ($w_t = f(w_d v_d^2)$), radial tracheid diameter ($d_r = f(w_d v_d^2)$), tangential tracheid diameter, fibre coarseness, and specific surface area. Denoted by the superimposed dashed parallel lines are the 95% prediction limits for absolute error (Equation (10), Table 5).

Specifically, as presented in Figure 2, the parameterized regression relationship for the attributes that attained statistical significance (m_e , w_d , m_a , w_t , d_r , c_o , and s_a) was also superimposed on the respective subgraph. Examination of these subgraphs indicated that the parameterized models were representative of the linear trends between the observational pairs, and devoid of any clear systematic bias. Additionally, the subgraph for d_t , which was not successfully parameterized, reconfirmed the statistical result: i.e., there was no definitive linear or nonlinear trend evident for the 61 $d_t - w_d v_d^2$ observational pairs. The magnitude and pattern of the absolute biases for each relationship as presented in Figure 3 (residual plots) also confirmed that the significant relationships were devoid of consequential outliers and systematic bias across predictor variable values.

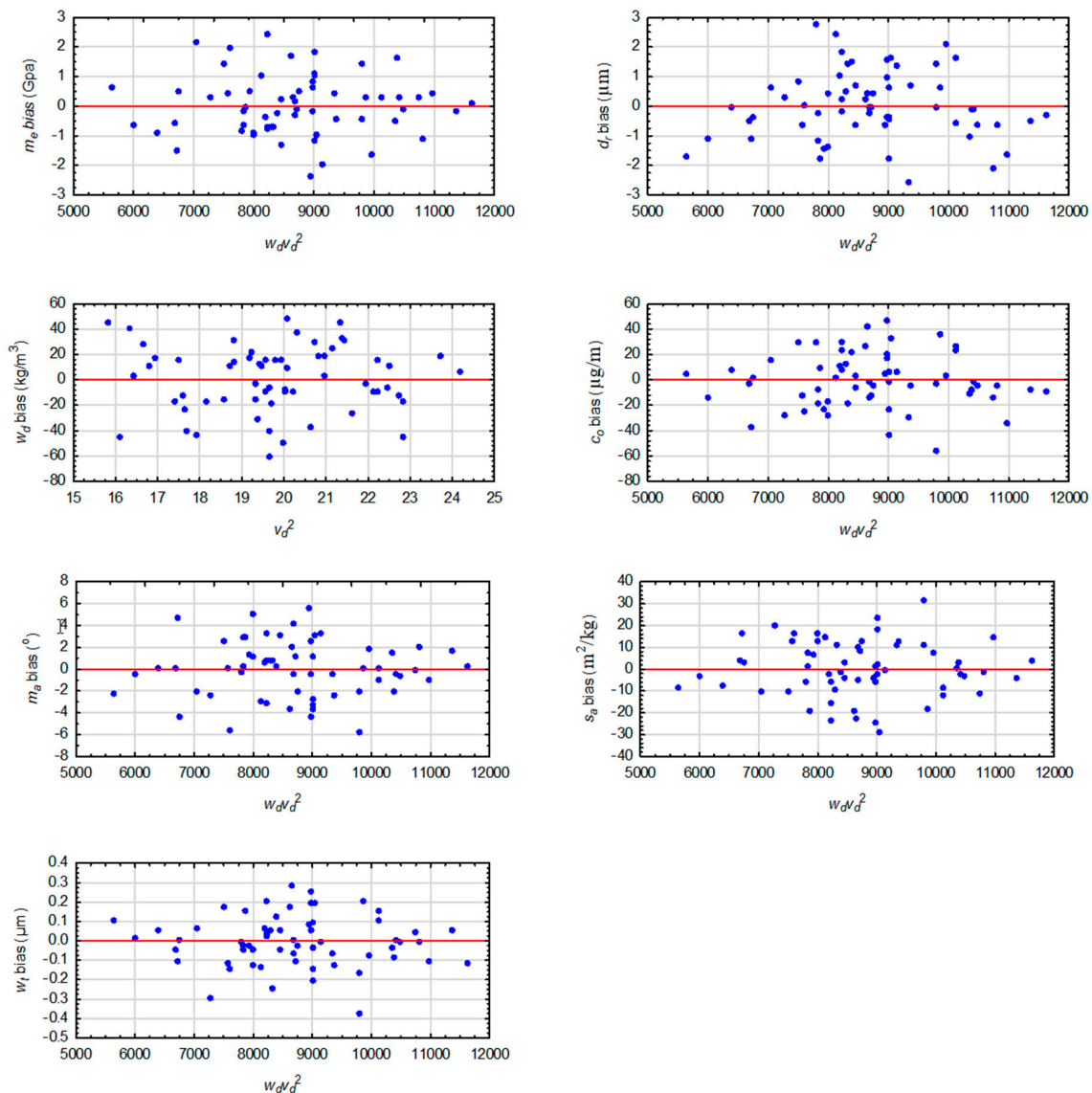


Figure 3. Attribute-specific absolute bias (residual) plots for significant ($p \leq 0.05$) regression relationships (Table 4, Figure 2).

The prediction and tolerance intervals that provide the probable range of absolute and relative biases when the regression equations are used to predict attribute estimates for a new sampled tree, are presented in Table 5.

Accordingly, the absolute errors arising from the m_e , m_a , w_t , d_r , c_o , and s_a equations when deploying an acoustic velocity measurement along with a Silviscan-equivalent wood density estimate when applicable for a newly sampled jack pine tree, would be expected to fall within the following

attribute-specific absolute intervals: (1) $-2.0 \leq m_e$ error (GPa) ≤ 2.0 , $-52.4 \leq w_d$ error (kg/m^3) ≤ 52.4 , $-5.3 \leq m_a$ error ($^\circ$) ≤ 5.3 , $-0.3 \leq w_t$ error (μm) ≤ 0.3 , $-2.3 \leq d_r$ error (μm) ≤ 2.3 , $-40.8 \leq c_o$ error ($\mu\text{g/m}$) ≤ 40.8 , and $-25.6 \leq s_a$ error (m^2/kg) ≤ 25.6 . Similarly, the corresponding relative errors would be expected to fall within the following attribute-specific percentage-based intervals (Table 5): $-17.1 \leq m_e$ error (%) ≤ 18.5 ; $-11.6 \leq w_d$ error (%) ≤ 12.4 , $-37.5 \leq m_a$ error (%) ≤ 44.7 , $-9.0 \leq w_t$ error (%) ≤ 9.4 , $-7.5 \leq d_r$ error (%) ≤ 7.7 , $-9.9 \leq c_o$ error (%) ≤ 10.3 , and $-8.2 \leq s_a$ error (%) ≤ 8.6 . The 95% confidence limits for an absolute prediction error within the context of the data range for the composite independent variable, are also exemplified in the subgraphs within Figure 2.

The tolerance interval, which has a greater width than that of the corresponding prediction error interval, infers that there is a 95% probability that 95% of all future errors will fall within the stated interval. Accordingly, the absolute errors arising from the m_e , m_a , w_t , d_r , c_o , and s_a equations when deploying an acoustic velocity measurement along with a Silviscan-equivalent wood density estimate when applicable, 95% of all future absolute biases would fall within the following attribute-specific intervals (Table 5): $-2.4 \leq m_e$ error (GPa) ≤ 2.4 , $-60.5 \leq w_d$ error (kg/m^3) ≤ 60.5 ; $-6.1 \leq m_a$ error ($^\circ$) ≤ 6.1 , $-0.3 \leq w_t$ error (μm) ≤ 0.3 , $-2.7 \leq d_r$ error (μm) ≤ 2.7 , $-47.2 \leq c_o$ error ($\mu\text{g/m}$) ≤ 47.2 , and $-29.6 \leq s_a$ error (m^2/kg) ≤ 29.6 . Similarly, the corresponding relative errors would be expected to fall within the following attribute-specific intervals (Table 5): $-19.8 \leq m_e$ error (%) ≤ 21.2 , $-13.5 \leq w_d$ error (%) ≤ 14.2 , $-43.8 \leq m_a$ error (%) ≤ 51.0 , $-10.5 \leq w_t$ error (%) ≤ 10.9 , $-8.6 \leq d_r$ error (%) ≤ 8.8 , $-11.5 \leq c_o$ error (%) ≤ 11.9 , and $-9.5 \leq s_a$ error (%) ≤ 9.9 . As evident from the width of the prediction and tolerance error intervals for relative errors, the regression relationships did vary considerably in terms of their predictive ability. For example, the relationship for m_a exhibited a much larger width than those associated with the m_e , w_d , w_t , d_r , c_o , and s_a relationships. Notably, however, all seven relationships exhibited no evidence of prediction bias and, thus, all would generate unbiased attribute estimates when deployed to newly sampled jack pine trees, albeit at varying levels of precision.

3.2. Parameterized Amplitude-Wood Density Model for Jack Pine

The parameter estimates, regression statistics, and the prediction error intervals for the mean amplitude—density relationship (Equation (6)) are given in Table 6. Figure 4 graphically illustrates the relationship in context of the $w'_d - a_m$ observational pairs used to parameterize the model. Overall, the regression model described a moderate level (51%) of the total variation in density (i.e., $r^2 = 0.51$). The residual analyses indicated that there was insufficient evidence to reject the OLS assumptions of homogeneity of variance and normality. Likewise, there was no systematic biasedness or lack-of-fit issues associated with the parameterized relationship. Specifically, a visual interpretation of the regression equation within the context of the $w'_d - a_m$ observational pairs revealed that the relationship followed the general linear trend of the data pairs and was devoid of consequential outliers (Figure 4). Similarly, the mean absolute and relative mean biases and their associated 95% confidence intervals were not significantly different from zero and, hence, no lack-of-fit was evident (Table 6). The prediction interval indicated that there is a 95% probability that the bias from a single future prediction will be within $\pm 51 \text{ kg/m}^3$ or $\pm 12\%$ of the true density value whereas the tolerance interval indicated that there is a 95% probability that 95% of all future biases will be within $\pm 57 \text{ kg/m}^3$ or $\pm 13\%$ of their true density values. The 95% confidence limits for the absolute prediction error within the context of the data range from the observational pairs used to parameterize the relationship, are also graphically illustrated in Figure 4.

Table 6. Parameter estimates, regression statistics, and predictive bias intervals for the relationship between mean amplitude and wood density.

Parameter Estimates and Regression Statistics						Lack-of-Fit Measures ^c				Predictive Ability: 95% Error Intervals ^d			
Parameter Estimates ^a		Regression Statistics ^b				Absolute		Relative (%)		Prediction		Tolerance	
Intercept	Slope	<i>df</i>	<i>r</i> ²	<i>SEE</i>	<i>F</i> -Ratio	Mean	95%	Mean	95%	Absolute	Relative	Absolute	Relative
		<i>(n_{reg}, n_{res})</i>		(kg/m ³)		Bias	CL	Bias	CL	95% CL	95% CL	95% CL	95% CL
360.524	4.378	1119	0.506	25.753	122.1 *	0.00	±4.62	0.33	±1.04	±51.00	±11.5	±56.53	±12.8

Note: Absolute and relative lack-of-fit and predictive ability measures are in units of kg/m³ and %, respectively. a: OLS parameter estimates for the intercept (β_0) and slope (β_1) (Equation (6)). b: As defined in Table 4. c: Mean absolute (Equation (7)) and relative (Equation (8)) bias and the limits (CL) of the associated 95% confidence interval (Equation (9)) where mean values not significantly ($p > 0.05$) different from zero were indicative of an unbiased relationship. d: 95% prediction and tolerance error limits (CL) for absolute and relative errors (Equations (10) and (11), respectively): mean bias \pm 95% CL. Specifically, there is a 95% probability that a future error will be within the stated prediction interval and that there is a 95% probability that 95% of all future errors will be within the stated tolerance interval [42,43].

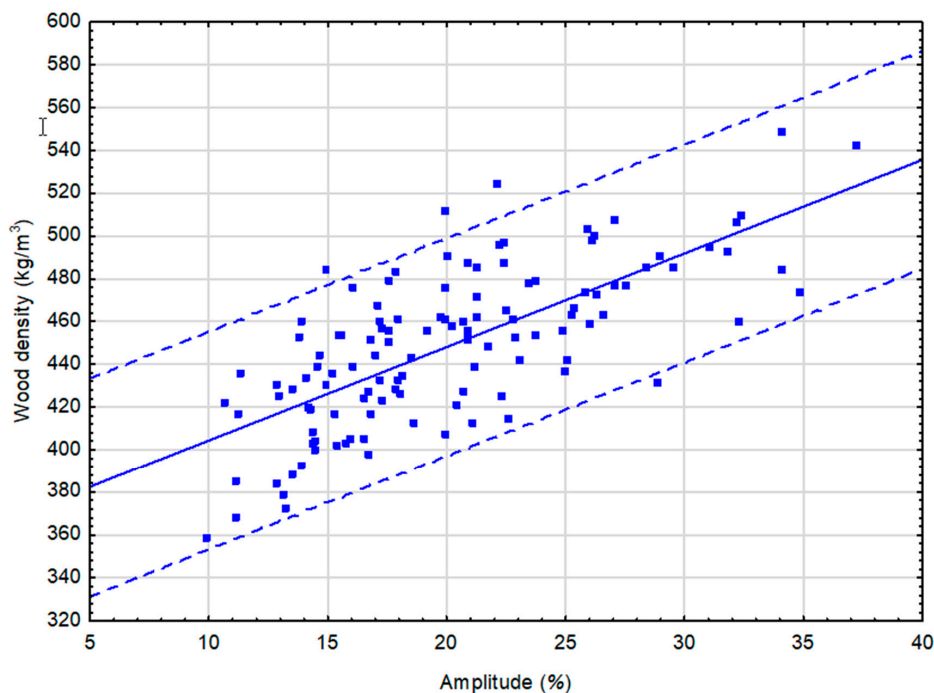


Figure 4. Relationship between mean amplitude and wood density with the significant ($p \leq 0.05$) regression relationship superimposed (solid line, Equation (6), Table 6). Denoted by the superimposed dashed parallel lines are the 95% prediction limits for absolute error (Equation (10), Table 6).

3.3. Predictive Performance of the Fibre Attribute Prediction Models when Deploying an Acoustic-Based Wood Density Estimate

The predictive performance metrics presented in Table 5 are applicable when a Silviscan-based estimate of wood density is used. Realistically, however, such estimates would not be normally available when field sampling and, hence, alternative methods of estimating the prerequisite wood density value for a newly sampled standing jack pine tree are required. The results of this study offer two possible solutions: (1) using an acoustic-based estimate by deploying the parameterized relationship developed for wood density as provided in Table 4 ($w_d = f(\hat{\beta}_{0,1}, \hat{v}_d^2)$), or (2) using a Resistograph-based estimate derived from the parameterized relationship given in Table 6 ($w_d = f(\hat{\beta}_{0,1}, a_m)$). Although the available data did not allow the latter relationship to be evaluated in terms of quantifying the magnitude of the prediction error to be incurred when used, it did allow the former scenario to be assessed. Analytically, this involved deploying an acoustic-based wood density estimate as a surrogate measure for the Silviscan-based estimate and generating the corresponding attribute estimates for each sample tree: i.e., $m_e, m_a, w_t, d_r, c_o, s_a = f(\hat{\beta}_{0,1}, \hat{w}_d \hat{v}_d^2)$ where \hat{w}_d is derived from the $w_d = f(\hat{\beta}_{0,1}, \hat{v}_d^2)$ relationship. These resultant predictions along with the observed values were used to derive prediction and tolerance error intervals for both absolute and relative error. Additionally, given that the expected relative error for some of the attributes when the parameterized equations are applied to individual trees would most likely exceed the precision requirements of most potential end-users (e.g., $\pm 18\%$ error for the modulus of elasticity even when using a Silviscan-equivalent wood density estimate, Table 5), the mean prediction errors arising from a group-based (stand-level) sampling strategy were also included. Hence, this supplementary assessment of deploying an acoustic-based density estimate consisted of calculating (1) the 95% confidence, prediction, and tolerance intervals for absolute and relative biases arising from sampling a single new tree where $n_p = 1$, and (2) the 95% prediction error interval for absolute and relative biases arising from sampling a group trees ($n_p = 30$). The results from this dual assessment indicated that this approach would provide unbiased estimates irrespective of the error type (i.e., the mean absolute and relative biases were not significantly ($p \leq 0.05$) different from zero, as inferred from the 95% confidence intervals, Table 7).

Table 7. Predictive performance measures for relationships utilizing an acoustic-based wood density estimate.

Relationship	Lack-of-Fit Measures ^a				Predictive Ability: 95% Error Intervals ^c			
	Absolute ^b		Relative (%)		Prediction (Stand-Level)		Tolerance	
	Mean Bias	95% CL	Mean Bias	95% CL	Absolute ^b 95% CL	Relative (%) 95% CL	Absolute ^b 95% CL	Relative (%) 95% CL
$m_e - w_d v_d^2$	0.002	±0.294	0.948	±2.526	±2.311 (±0.511)	±19.89 (±4.40)	±2.669	±22.97
$m_a - w_d v_d^2$	−0.003	<u>±0.628</u>	2.059	<u>±4.915</u>	±4.943 (±1.093)	<u>±38.70</u> (±8.51)	±5.708	<u>±44.68</u>
$w_t - w_d v_d^2$	0.003	±0.047	0.466	±1.720	±0.364 (±0.081)	±13.43 (±2.98)	±0.421	±15.53
$d_r - w_d v_d^2$	0.001	±0.308	0.149	±1.011	±2.426 (±0.537)	±7.96 (±1.76)	±2.801	±9.19
$c_o - w_d v_d^2$	0.270	±6.154	0.365	±1.528	±48.061 (±10.658)	±11.94 (±2.65)	±55.557	±13.80
$s_a - w_d v_d^2$	0.000	±4.561	0.269	±1.494	±35.915 (±7.944)	±11.76 (±2.60)	±41.468	±13.58

a: Mean absolute (Equation (7)) and relative (Equation (8)) bias and the limits (CL) of the associated 95% confidence interval (Equation (9)) where mean values not significantly ($p > 0.05$) different from zero were indicative of an unbiased relationship. b: Absolute error units are attribute-specific: GPa, °, μm, μm, μg/m and m²/kg for m_e , m_a , w_t , d_r , c_o , and s_a , respectively. c: Confidence limits (CL) for the 95% prediction and tolerance error intervals for absolute and relative errors (Equations (10) and (11), respectively): mean bias ± 95% CL. Specifically, there is a 95% probability that a future error will be within the stated prediction interval and that there is a 95% probability that 95% of all future errors will be within the stated tolerance interval [42,43]. For the stand-level prediction intervals, there is a 95% probability that the mean error generated from sampling 30 new trees will be within the stated prediction interval. Underlined values denote approximate values given non-normality of the error distributions at the 0.05 probability level.

In terms of precision, the prediction error intervals indicated that there was a 95% probability that a future error arising from the prediction of m_e , m_a , w_t , d_r , c_o , and s_a by using a newly acquired acoustic velocity measurement for an individual jack pine tree along with the corresponding acoustic-derived density estimate, would fall within the following attribute-specific absolute intervals (Table 7): $-2.3 \leq m_e$ error (GPa) ≤ 2.3 , $-4.9 \leq m_a$ error ($^\circ$) ≤ 4.9 , $-0.4 \leq w_t$ error (μm) ≤ 0.4 , $-2.4 \leq d_r$ error (μm) ≤ 2.4 , $-48.3 \leq c_o$ error ($\mu\text{g}/\text{m}$) ≤ 48.3 , and $-35.9 \leq s_a$ error (m^2/kg) ≤ 35.9 . Similarly, on a relative basis, the corresponding relative prediction error would be expected to fall within the following attribute-specific intervals: $-18.9 \leq m_e$ error (%) ≤ 20.8 , $-36.6 \leq m_a$ error (%) ≤ 40.8 , $-13.0 \leq w_t$ error (%) ≤ 13.9 , $-7.8 \leq d_r$ error (%) ≤ 8.1 , $-11.6 \leq c_o$ error (%) ≤ 12.3 , and $-11.5 \leq s_a$ error (%) ≤ 12.0 .

In accord with expectation, the precision of the estimates increased dramatically when assessed at the stand-level. Specifically, the prediction error intervals for estimating the mean from a group of trees indicated that there was a 95% probability that the mean error arising from the prediction of m_e , m_a , w_t , d_r , c_o , and s_a by using newly acquired acoustic velocity measurements from a sample of 30 jack pine trees, along with their corresponding acoustic-derived density estimates, would fall within the following absolute and relative intervals (Table 7): (1) $-0.5 \leq m_e$ mean error (GPa) ≤ 0.5 , $-1.1 \leq m_a$ mean error ($^\circ$) ≤ 1.1 , $-0.1 \leq w_t$ mean error (μm) ≤ 0.1 , $-0.5 \leq d_r$ mean error (μm) ≤ 0.5 , $-10.9 \leq c_o$ mean error ($\mu\text{g}/\text{m}$) ≤ 10.4 , and $-7.9 \leq s_a$ mean error (m^2/kg) ≤ 7.9 , and (2) $-3.5 \leq m_e$ mean error (%) ≤ 5.3 , $-6.5 \leq m_a$ mean error (%) ≤ 10.6 , $-2.5 \leq w_t$ mean error (%) ≤ 3.4 , $-1.6 \leq d_r$ mean error (%) ≤ 1.9 , $-2.3 \leq c_o$ mean error (%) ≤ 3.0 , and $-2.3 \leq s_a$ mean error (%) ≤ 2.9 .

The tolerance error intervals indicated that there was a 95% probability that 95% of all future errors generated from the use of an acoustic-derived density estimate in the m_e , m_a , w_t , d_r , c_o , and s_a equations would fall within the following attribute-specific intervals: $-2.7 \leq m_e$ error (GPa) ≤ 2.7 , $-5.7 \leq m_a$ error ($^\circ$) ≤ 5.7 , $-0.4 \leq w_t$ error (μm) ≤ 0.4 , $-2.8 \leq d_r$ error (μm) ≤ 2.8 , $-55.3 \leq c_o$ error ($\mu\text{g}/\text{m}$) ≤ 55.8 , and $-41.5 \leq s_a$ error (m^2/kg) ≤ 41.5 . On a relative basis, the corresponding tolerance intervals indicate that 95% of all future errors would fall within the following attribute-specific intervals: $-22.0 \leq m_e$ error (%) ≤ 23.9 , $-42.6 \leq m_a$ error (%) ≤ 46.7 , $-15.1 \leq w_t$ error (%) ≤ 16.0 , $-9.0 \leq d_r$ error (%) ≤ 9.3 , $-13.4 \leq c_o$ error (%) ≤ 14.2 , and $-13.3 \leq s_a$ error (%) ≤ 13.8 . Collectively, these absolute and relative prediction and tolerance error intervals, indicated that the parameterized models when deploying an acoustic-derived wood density estimate, would generate unbiased estimates irrespective of the attribute under consideration. However, the level of precision would vary substantially among the attributes ($d_r > s_a > c_o > w_t > m_e \gg m_a$) and by the sampling approach employed (stand > tree).

4. Discussion

The diverse array of end-products, which jack pine yields upon harvest [25], suggest that in-forest forecasting of end-product potential could lead to important operational advancements in terms of informing product-based inventories, enabling the identification and prioritization of stands for harvest according to real-time market-driven requirements or existing capabilities of conversion centres, improving value recovery, and enhancing overall segregation and merchandizing efficiency. Historically, a range of approaches for estimating end-product potential of standing trees and harvested logs have been advanced [5]. Non-invasive methods based on the deployment of external tree and log morphological-based indices to infer end-product potential have generated mixed results [44–46]. For example, external characteristics such as stem size (diameter, height, and taper) and crown dimensional variables (diameter and length) have been shown to be significantly related to a number of key internal wood characteristics, which underlie end-product type and quality. However, the explanatory power of the derived prediction models has been weak. Multiple regression models developed for a suite of Silviscan-derived attributes (m_e , w_d , m_a , d_r , d_t , and c_o) for 495 white spruce (*Picea glauca* (Moench) Voss) trees, which deployed tree size and crown dimensional predictor variables, were only able to explain no more than 13% of the variation for any of the key attributes (m_e , m_a , and w_d , [45]). Somewhat better results were reported by Kuprevicius [46] who found that similarly

structured regression-based models for a sample of 43 white spruce trees could explain 50% of the variation in the static modulus of elasticity.

Invasive methods including the deployment of destructive methods such as the extraction of increment cores followed by their Silviscan processing, yield explicit attribute estimates that can be used directly to infer end-product potential without consequential error or bias [29]. Although such invasive methods are widely used in silvicultural-based research investigations [47], the logistical challenges, and the time and fiscal commitments required to implement this approach, have largely negated its operational deployment in pre-harvest assessments of end-product potential [5]. By contrast, non-invasive acoustic-based approaches in which commercially-relevant attributes can be estimated on-site, in real-time, and at sufficiently lower cost than invasive methods, represent a viable alternative for forecasting end-product potential [24]. However, the limited scope of the traditional acoustic-based inferential framework, species-specific nature of acoustic-based attribute relationships, and the general lack of associated performance measures in terms of the degree of bias and predictive precision, warranted a further in-depth prerequisite examination of these issues. Hence, the consequential importance of the results presented in this study in terms of solidifying and advancing the potential utility of the acoustic approach in boreal forest management, albeit for a single species (jack pine).

4.1. Fibre Attribute-Specific Acoustic Velocity Relationships for Standing Jack Pine Trees and Sampling Considerations

The results for the jack pine trees assessed in this study indicated that the proportion of variation explained by the linear regression specification varied by attribute. The highest level of explanatory power was found to be associated with the primary relationship ($m_e = f(w_d v_d^2)$) in which 71% of the variation in the dynamic modulus of elasticity was explained, as quantified by the coefficient of determination ($r^2 = 0.71$, Table 4). This result exceeds that of Chen [48] for standing Norway spruce (*Picea abies* (L.) Karst.) trees who reported a r^2 -equivalent value of 0.28 based on a simple linear regression model specification. Likewise, these results for jack pine exceed those reported by Newton [14] for standing red pine trees (i.e., r^2 value of 0.40). Other studies, which evaluated the relationship between acoustic velocity of standing trees and the static modulus of elasticity of clear xylem samples or resultant end-products (e.g., sawn boards) employing a regression model specification that omitted the wood density term ($m_e = f(v_d^2)$), have produced largely mixed results. For example, Amateis and Burkhart [49] found no statistically significant ($p \leq 0.05$) relationship for standing loblolly pine (*Pinus taeda* L.) trees. However, for standing Norway spruce trees, Fischer [50] found a weak but significant ($p \leq 0.05$) relationship ($r^2 = 0.13$). Moderate levels of explanatory power (mean $r^2 = 0.44$) and significant ($p \leq 0.05$) relationships were reported for standing Sitka spruce (*Picea sitchensis* (Bong.) Carr.) and western hemlock (*Tsuga heterophylla* (Raf.) Sarg.) trees by Wang [51]. Nanami [52] also found a significant ($p \leq 0.05$) relationship with a moderately high level of explanatory power ($r^2 = 0.59$) for standing Sugi (*Cryptomeria japonica* D. Don.) trees.

Apart from the results provided for red pine trees by Newton [14], published results for the secondary attribute—acoustic velocity relationships examined in this study have been largely limited to examining acoustic-based relationships pertaining to the prediction of microfibril angle and wood density [9,53]. Based on an assessment of the same suite of acoustic-based relationships investigated in this study but for red pine, similar but not identical results were obtained. Specifically, deploying Silviscan-based attributes and time-of-flight acoustic velocity measures from 54 red pine trees, statistically significant ($p \leq 0.05$) regression relationships were obtained for m_e , w_d , w_t , c_o , and s_a . Along with the two additional attribute relationships that could be established for jack pine but not for red pine (m_a and d_r), the portion of variability explained was greater for the jack pine relationships than that for the corresponding red pine relationships. Specifically, 40% of the variation was explained in the dynamic modulus of elasticity for red pine versus 71% for jack pine, 14% of variation was explained in wood density for red pine versus 30% for jack pine, 45% of the variation was explained in cell wall thickness for red pine versus 66% for jack pine, 27% of the variation was explained in fibre coarseness

for red pine versus 42% for jack pine, and 43% of the variation was explained in specific surface area for red pine versus 61% for jack pine. However, in terms of predictive precision, the relationships for red pine were slightly more precise than those observed in jack pine. This was attributed to the greater inherent variability in the attribute values for the jack pine trees relative to the those for red pine trees. For example, attribute-specific coefficients of variation for the 61 jack pine sample trees (Table 1, this study) were approximately twice that of red pine (see Table 3 in Newton [14]). Red pine is a more genetically invariant species relative to jack pine, which may partially explain the difference in the magnitude of attribute variation between the two species (sensu [25]).

Study variation among the attribute—acoustic velocity relationships is also not unexpected given differences among investigations in terms of sampling procedures, analytical approaches, instrumentation, species, and locale. Furthermore, internal tree factors such as variation among sample trees in knot distributions, embedded voids, growth rates, temperature and moisture conditions of the xylem when measured, and external factors such as tree size, local competition around the sampled tree, and site conditions, are also potential sources of error that could contribute to the degree of unexplained variation and reduced the statistical significance of the attribute—acoustic velocity relationships [54–56]. Thus yielding the approach used in this study, which attempted to minimize some of these known sources of variation: i.e., (1) usage of Silviscan-based attributes measured from xylem tissue sequences extracted via destructive stem analysis from standing-trees upon felling, (2) employment of a single calibrated acoustic sampling device for all sample trees, (3) systematic measurement of acoustic velocities at multiple circumferential positions, (4) selecting sampling trees from stands growing on similar site productivities, at equivalent stages of maturity, and with similar silvicultural histories, and (5) collecting acoustic velocity measurements during identical seasonal periods (early autumn). Nevertheless, the resultant regression relationships for jack pine could achieve only an overall moderate level of explanatory power.

One of the prime determinates underlying the potential deployment of in-forest acoustic-based attribute forecasting is the degree of precision required by the end-user. Differentiating individual standing trees by end-product potential, according to narrow design-based thresholds, requires a high degree of predictive accuracy. Quantitatively, the residual mean square errors along with the prediction and tolerance error intervals, provide insight into the predictive performance of the relationships when potentially deployed. Although the lack of attribute-specific design threshold values that can be explicitly linked to end-product potential hinders the ability to provide conclusive guidance on interpreting the acoustic-generated attributes, an examination of existing grading manuals for some of the potential end-product categories for softwood species can be informative (sensu [14]). For example, threshold values for the modulus of elasticity associated with a specific lumber grade have been defined for machine stress-rated dimensional lumber products. The mean difference in the static modulus of elasticity value across 14 machine stress-rated lumber grades is approximately 0.7 GPa [16]. The mean standard error of the estimate for the relationship between the dynamic modulus of elasticity and density-weighted acoustic velocity for jack pine is approximately 1.0 GPa. Furthermore, the corresponding error intervals suggest the 95% of future predictions for newly sample jack pine trees would have a range of ± 2.4 GPa when using a Silviscan-equivalent wood density estimate (Table 5) and ± 2.7 GPa when using an acoustic-derived wood density estimate (Table 7). These precision metrics suggest that the acoustic-based m_e estimate would not be accurate enough to differentiate among these narrow grade classes, even if it is assumed that the m_e within a standing tree is equivalent to that in its derived dimensional lumber product. However, combining the grade categories into a smaller set of discrete product grade classes may assist in overcoming this issue, depending on the within-class ranges used. For example, based on the NLGA [14] machine stress-rated lumber specifications for spruce, pine, and fir boards, Paradis [57] delineated three m_e -based grade classes to represent lumber end-product potentials for black spruce. These three classes, denoted low, medium, and high grade, were differentiated by approximately 1.5 m_e units (GPa). Thus, if similarly applied to the jack pine, the dynamic m_e estimate would still, however, not be precise enough to

segregate an individual tree into one of these three classes (i.e., given the ± 2.7 GPa expected error associated with each m_e prediction). Consequently, increasing the class threshold widths, which would reduce the number of groupings, may be required with respect to segregating individual standing jack pine trees in specific grade classes.

Alternatively, stand-level sampling in which acoustic velocity and associated wood density estimates are obtained from a group of trees may be precise enough to yield a mean m_e estimate accurate enough to differentiate stands, according to their end-product potential. For example, the mean m_e estimate derived from acoustic velocity measurements from 30 trees within a stand along with acoustic-based density estimates, would be within ± 0.5 GPa of the true mean value (Table 7). Thus, in this case, the level of accuracy attained at the stand-level would be precise enough to segregate stands into one of the three grade classes based on the within-class m_e range proposed by Paradis [57]. Potentially, scaling acoustic-based stand-level mean attribute estimates to the forest level by integrating remotely-sensed forest inventory information could also be of utility when attempting to generate landscape-level wood quality property maps [57,58].

The expansion of the primary m_e - v_d relationship resulted in the derivation of additional secondary acoustic—attribute relationships that may be of utility in the non-destructive estimation of end-product potentials of standing trees. Newton [14] employed a similar experimental and analytical approach as what was used in this study to assess attribute—acoustic velocity relationships for standing red pine trees. Results of that analysis revealed significant ($p \leq 0.05$) regressions for five of the eight attributes studied (m_e , w_d , w_t , c_o , and s_a) with slightly lower performance metrics in terms of explanatory power and predictive ability. Although references to other studies employing a similar analytical framework are not readily apparent within the literature, the empirical findings presented for red pine and jack pine provide confirmatory evidence in support of the proposed acoustic-based inferential framework. For these additional attributes, such as wood density, microfibril angle, tracheid wall thickness, radial tracheid diameter, fibre coarseness, and specific surface area, similar issues arise as that discussed above regarding the interpretation of the modulus of elasticity estimates. Although the lack of direct linkages between within-tree attributes estimates and those within finished end-products limits the ability to identify and classify standing jack pine trees into discrete end-product categories, using the suite of attribute estimates could, nevertheless, provide sufficient guidance to stratify individual trees or stands into general end-product categories. Trees or stands with high stiffness and density values could be associated with having a greater potential to produce higher grade solid-wood end-products relative to those with corresponding lower values (sensu [4]). Similarly, trees or stands with larger tracheid wall thickness and fibre coarseness values, could be inferred as having a greater potential to produce higher quality pulp and paper end-products than trees or stands with corresponding smaller values (sensu [4]).

In terms of field sampling, recent results examining the effect of xylem temperature and moisture on acoustic velocity within standing semi-mature jack pine trees during the vegetative growing season, indicated that, although xylem moisture had no appreciable influence, acoustic velocity did decline in a linear fashion with increasing temperature [59]. However, the temperature effect was not of consequential significance except when xylem temperatures approached their seasonal extremities (minimums (< 5 °C) and maximums (> 30 °C)). Consequently, this source of variation could be considered as random error provided that temperatures did not exceed these thresholds when acoustic sampling. Otherwise, the correction equation for standardizing acoustic velocities to a reference xylem temperature (20 °C), as provided in Newton [59], could be utilized.

4.2. Non-Destructive Wood Density Estimation and Consequences on Its Use in Fibre Attribute Predictions

Irrespective of the magnitude of the portion of variability explained and with the exception of the relationship for the tangential tracheid diameter, the results of this study demonstrated that the in-forest acoustic approach could provide unbiased estimates of the dynamic modulus of elasticity, wood density, microfibril angle, tracheid wall thickness, radial tracheid diameters, fibre coarseness,

and specific surface area, within standing jack pine trees. In accord with the parameterized primary and derived secondary acoustic-based relationships, estimates of wood density would be required for their operational deployment. The results of this study provide two potential non-destructive methods that could be used. Specifically, utilizing the wood density estimate derived from (1) an acoustic velocity measurement obtained using a time-of-flight tool (Director ST300) in combination with the $w_d = f(v_d^2)$ parameterized regression equation (Equation (5b), Table 4), or (2) a drill resistance mean amplitude measurement obtained from the Resistograph profile in combination with the parameterized $w_d = f(a_m)$ regression equation (Equation (6), Table 6). With respect to the latter method, previous studies have reported varying degrees of association between the mean amplitude values derived from micro-drilling resistance tools, such as the Resistograph, and wood density within standing trees. For example, Isik and Li [60] reported a phenotypic-based correlation of 0.75 for eight-year-old loblolly pine (*Pinus taeda* L.) clones. This would translate into an approximate coefficient of determination value of 0.56 based on a simple linear regression relationship, which is not dissimilar to that reported in this study ($r^2 = 0.51$, Table 6). Employing a similar but not identical analytical approach but for red pine trees, Newton [14] reported a statistically significant ($p \leq 0.05$) mean amplitude-wood density relationship for red pine trees. However, the portion of variability explained was lower than what was determined for jack pine (27% for red pine versus 51% for jack pine). Downes [61] reported viable relationships for five eucalypt plantations (*Eucalyptus globulus* Lambill. ($n = 4$), and *Eucalyptus nitens* (Deane & Maiden) Maiden ($n = 1$)) located in Northwest Tasmania ($n = 2$) and Western ($n = 2$) and South-Eastern Australia ($n = 1$). Deploying a simple linear model similar in specificity to that employed in this study for the five separate plantations, Downes [61] reported statistically significant ($p \leq 0.05$) mean amplitude-wood density relationships, which explained a moderate to high level of core-based density (e.g., coefficients of determination ranging from 0.66 to 0.87). Although intercept and slope values were generally stable and of similar magnitude across the sampling sites, slight differences were observed, particularly with regard to the slope term. Downes [61] suggested that instrumentation-induced variation and sampling conditions were plausible determinates underlying these differences.

In consideration of the empirical evidence as provided in this jack pine study and those from past investigations [57,58], along with the results from analytical-based comparative assessments examining the performance of competing technologies (direct-based increment core extraction methods and indirect-based impact approaches, [62]), it is evident that the drill resistance approach is a viable in-forest method for non-destructively estimating wood density. Logistically, however, when comparing the micro-drill resistance and acoustic-based approaches, the former approach would be more challenging to implement given the requirement for additional on-site equipment (Resistograph) and data management (i.e., on-site editing of profile output data streams in order to calculate a mean amplitude value for the xylem portion of the stem). For jack pine, the wood density estimate obtained via resistance drilling would only be marginally more precise than the acoustic-based estimate: approximately 1% to 2% increase in absolute width of the relative error intervals obtained via resistance drilling over that obtained through acoustic-sampling (cf. Tables 5 and 6). Although recent advancements in automating the processing of Resistograph profiles in terms of generating mean amplitude values have reduced the computational burden (i.e., web-based computational software [61]), the acoustic-based approach would be the most applicable for jack pine given that it requires the least amount of effort with regard to logistical requirements and data processing, provides a real-time on site density estimate, and is only marginally inferior in terms of predictive precision. Other low impact tools and techniques such as the mechanical-based Pilodyn impact device [63] and near infra-red spectrometers [64] could also be potentially used to estimate wood density non-destructively. However, assessing their utility and predictive performance was beyond the scope of this study.

The in-forest deployment of the acoustic-based prediction equations developed in this study will ultimately depend on the requirements of the end-user in terms of the accuracy of the point-estimate for a given attribute that is actually required. For example, if the relationships are used to stratify

individual standing trees into various product categories (e.g., solid wood products versus pulp and paper) and then assign a potential grade class within the categories (e.g., select or economy grade for dimensional lumber products), then information pertaining to the accuracy of the point-estimate will be of the utmost importance. The provision of predictive performance metrics for each of the parameterized relationships enables end-users to assess the potential utility of the acoustic approach in their pre-harvest value-based inventory assessments (e.g., predictive intervals demarks the error range generated when using the equations on a newly sampled tree). For example, deploying an acoustic-based wood density estimate, the magnitude of the error arising from a m_e , m_a , w_t , d_t , c_o , and s_a prediction would be expected to be within approximately $\pm 20\%$, $\pm 39\%$, $\pm 13\%$, $\pm 8\%$, $\pm 12\%$, and $\pm 12\%$ of their true values, respectively (Table 7). The intervals for a m_e and m_a are relatively large and, thus, would, in all likelihood, negate the ability to classify individual stand jack pine trees into narrow grade classes based on these two attributes. Alternatively, if the approach was used in the context of stand-level fibre attribute characterization in which acoustic sampling was conducted on a large number of individual trees within a given stand in order to generate a mean population-level estimate, then the stand-level prediction error intervals would be of the utmost importance. As shown in this study, the mean error arising from 30 m_e , m_a , w_t , d_t , c_o , and s_a predictions would be expected to be within approximately $\pm 4\%$, $\pm 9\%$, $\pm 3\%$, $\pm 2\%$, $\pm 3\%$, and $\pm 3\%$ of the true mean value, respectively (Table 7).

4.3. Relationship between Tree and Log Acoustic Velocities and its Utility in Generating a Poisson Ratio Estimate for Jack Pine

Functionally, the relationship between acoustic velocity and the dynamic modulus of elasticity for standing trees is different from that specified for harvested logs. The latter relationship is expressed as $m_{e(d)} = f(w_{d(f)}v_l^2)$ where v_l is the velocity of a mechanically-induced longitudinal stress wave (km/s). Logistically, the wave is created by hitting one of the log's open cross-sectional faces with an impact tool. The wave propagates through the log until it reaches the opposite cross-sectional face and then returns. A resonance-based acoustic instrument, which is also placed on the open cross-sectional face at the time of impact, measures the velocity of the wave as it transverses the xylem tissue within the log (e.g., Hitman HM200, Fibre-gen Inc.). Conversely, for standing trees, it is the velocity of a mechanically-induced dilatational or quasi-dilatational stress wave that enters the circumference of the stem just above stump height (0.5 m) through an inserted impact probe which passes vertically through the xylem tissue transecting breast-height (1.3 m) and is circumferentially measured at a stem height of approximately 1.5 m via the upper-positioned receiving probe (e.g., Director ST300 as was used in this study; Figure 1). Although the wave types differ along with their functional relationship with the modulus of elasticity, the velocity measurements have been shown to be empirically correlated.

More specifically, based on a simple linear regression model specification that was used to describe the relationship between v_l (dependent) and v_d (independent) for five coniferous species, Wang [12] reported significant ($p \leq 0.05$) relationships with moderate to high levels of explanatory power (r^2 values of 0.93, 0.85, 0.71, 0.83, and 0.90 for Sitka spruce (*Picea sitchensis* (Bong.) Carr.), western hemlock (*Tsuga heterophylla* (Raf.) Sarg), jack pine, ponderosa pine (*Pinus ponderosa* Dougl. ex Laws.), and radiata pine (*Pinus radiata* D. Don), respectively). Deploying v_l and v_d measurements for the trees and accompanying 1st-order butt logs (≈ 0 –20% height percentiles) for the trees used in this study, revealed a similar significant ($p \leq 0.05$) relationship with an approximately identical r^2 value (0.70) to that reported by Wang [12] for jack pine ($r^2 = 0.71$). This degree of concordance of the velocity correlative relationships for standing trees and derived logs across multiple species, provides a measure of confirmatory support for the acoustic approach in terms of its overall consistency and agreement with expectation. Furthermore, Wang [12] proposed that the ratio between v_d and v_l could be used to characterized species-specific differences between the wave types. Specifically, the mean v_d/v_l value across the five coniferous species assessed by Wang [12] ranged from 1.07 to 1.36 with a mean value of 1.20. Analyzing the jack pine trees sampled in this study revealed that the ratio ranged from 1.04 to

1.31 with a mean value of 1.24. Again, the species-specific ratio that was reported by Wang [12] for jack pine (1.21) was very similar to that obtained for the jack pine trees sampled in this study (1.24). More generally for conifers, calculating the mean ratio for all five species analyzed inclusive of the results of this study, suggest that the velocity of the dilatational wave measured in standing trees is approximately 1.22 times the velocity of the longitudinal wave measured in the derived logs.

The Poisson ratio (P) is used as a covariate in the functional relationship between the dynamic modulus of elasticity and density-weighted acoustic velocity within standing trees (Equation (1)). It is also an important mechanical property of wood since it measures the relative deformation in the vertical plane (expansion) with respect to the deformation in the horizontal plane (compression). More specifically, P is the transverse to axial strain ratio when a wood sample is axially loaded: the ratio of the deformation perpendicular to the direction of the load (transverse strain) relative to the degree of deformation parallel to the direction of the load (axial strain) [65]. Given that the ratio varies within and between species and is difficult to estimate without laboratory testing and analyses, the ratio is commonly treated as an unknown constant when acoustic sampling. Empirically, however, Wang [12] proposed an approach for generating species-specific Poisson ratio estimates deploying the ratio between tree-based v_d and log-based v_l measures. Mathematically, this involved three computational steps: (1) equating the $m_e = w_d v_l^2$ relationship developed for logs with the corresponding $m_e = ((1 + P)(1 - 2P)/(1 - P)) \cdot w_d v_d^2$ relationship developed for standing trees, yielding the expression, $w_d v_l^2 = ((1 + P)(1 - 2P)/(1 - P)) w_d v_d^2$, (2) given (1), simplifying and rearranging this expression yields a relationship in which the velocity ratio can be expressed as a function of the Poisson ratio, $v_d/v_l = ((1 - P)/(1 + P)(1 - 2P))^{0.5}$, and (3) given (2), deploying an empirical velocity ratio estimate for a given species yields a quadratic functional form, for which the positive root is taken as the Poisson ratio estimate. For example, employing the mean v_d value for the jack pine trees and mean v_l value obtained their extracted 1st-order butt logs, yields a velocity ratio value of 1.24 and the resultant quadratic function, $0.5376 - 0.5376P - 3.0752P^2$. Solving for P gives a positive root value of 0.34, that is, the estimated Poisson ratio for jack pine.

This derived estimated Poisson ratio for jack pine is almost identical to the one estimate derived by Wang [12] for their jack pine samples ($\hat{P} = 0.33$) and is not dissimilar to the one reported by Newton [14] for the red pine ($\hat{P} = 0.39$). Furthermore, calculating the mean P value from the values determined through mechanical testing on nine North American pine species (loblolly pine (*Pinus taeda* L.), lodgepole pine (*Pinus contorta* var. *latifolia*), longleaf pine (*Pinus palustris* P. Mill.), pond pine (*Pinus serotina* Michx.), ponderosa pine, red pine, slash pine (*Pinus elliottii* Engelm.), and western white pine (*Pinus monticola* Douglas ex D. Don)) as presented by Green [65], yielded a value of 0.34 (minimum/maximum/standard deviation = 0.28/0.39/0.03). Thus, the acoustic-based estimate for jack pine is not discordant with that derived through stress testing for the group of other commercially-important pine species grown in North America. The value is also equal to the mean value of 0.34 that is commonly assumed for both hardwood and softwood species (sensu [66]). An operationally plausible interpretation of the ratio is in terms of the plasticity of the xylem tissue of a given species to deform under pressure. For example, a ratio of 0.34 for jack pine, suggests that an upright piece of lumber would laterally expand approximately one-third as much as it would vertically compress when subjected to consequential axial loads. Based on a comparison of the acoustic-based Poisson estimates between species, suggest that red pine may exhibit a slightly greater rate of lateral deformity than jack pine when subjected to the same degree of axial compression (0.39 and 0.34 for red pine and jack pine, respectively). In addition to these generalized inferences, provision of a Poisson estimate provides a more complete description of the stiffness–acoustic velocity functional relationship, as represented by Equation (1).

4.4. Potential Utility of Acoustics in Value-Based Forest Management and Silvicultural Experimentation and Suggested Future Research Directions

Acoustic-based segregation of individual logs and trees based on wood quality characteristics and, by extension end-product potential within the upstream portion of the forest products supply chain, has been associated with increased operational efficiencies and associated profitability levels through the maximization of end-product value recovery [23]. Additionally, the acoustic approach has been shown to be of utility for silvicultural-based experimentation where acoustic-based attribute estimates are used as wood quality response surrogates to various density management treatments. For example, in a study on quantifying the thinning intensity effect on wood quality (density-weighted dynamic wood stiffness) in Calabrian pine (*Pinus nigra* Arnold subsp. *calabrica*) plantations in southern Italy, the acoustic approach was able to successfully differentiate treatment effects on end-product potential, which led to enhanced inference in terms of crop planning decision-making [67,68].

Recently, acoustic-based segregation analytics have undergone a period of rapid development for some intensely-managed and high-value pine species for which tree and log-based end-product estimation is considered fundamental to enhancing fiscal efficiency. Specifically, an acoustic-based generic segregation model developed for the tree-to-product portion of the forest products supply chain, has shown promise when parameterized for radiata pine in New Zealand [69]. Notationally referred to as SEGMOD, this techno-economic segregation model utilizes acoustic-based internal fibre estimates of standing tree measured during pre-harvest inventories and (or) harvested logs at the time of extraction (in-forest, landings, mill gate), along with terrain information, external characteristics, fixed and variable cost inputs, and mill configuration assumptions, to generate tree-level fiscal worth expectations based on a given market type. Empirical results arising from an extensive set of model simulations applied to four operational case studies throughout New Zealand, indicated that standing-tree and in-forest landing-based segregation yielded significantly greater fiscal returns ($\approx 10\%$) when compared to the results arising from the sorting yard, mill, and nil-based segregation scenarios.

Although similar analytical decision-support models have yet to be developed for boreal segregation operations, the results for jack pine provided in this study yields the prerequisite prediction equations for initiating such efforts. Furthermore, the scope of the acoustic-based attribute prediction relationships and overall inferential framework presented is much broader in terms of end-product-based fibre determinates. The results for standing jack pine trees empirically demonstrated that the acoustic approach could provide unbiased estimates of the dynamic modulus of elasticity, wood density, microfibril angle, tracheid wall thickness, radial tracheid diameters, fibre coarseness, and specific surface area. The jack pine relationships did, however, exhibit considerable variation in terms of the proportion of variation explained and predictive performance, which the error analyses revealed. Further research into plausible pathways that could reduce the amount of unexplained variation would be worthy of consideration. These efforts could include the identification and control of in-forest sources of systematic variation that negatively influences the attribute—acoustic velocity relationships [56], and the potential employment of a standardization procedure to account for the effects of xylem moisture and temperature variation on acoustic velocity if found to be significant [59,70]. Provision of end-product-specific design-based threshold values for the attributes assessed in this study would also advance the acoustic approach in terms of in-forest segregation operations. For example, enabling the differentiation of trees or stands, according to their end-product potential based on a specific range of design-based values for one or more of the studied attributes. Attaining a more complete understanding of the wave propagation pattern within the xylem tissue in terms of its cross-sectional coverage for the primary and derived secondary relationships, would also be constructive in advancing the acoustic approach in fibre attribute prediction and associated end-product forecasting.

5. Conclusions

The quality and associated economic value of manufactured wood-based end-products, such as dimensional lumber, engineered wood composites, and utility poles, are largely dependent on the characteristics of the internal fibre attributes within the merchantable portion of the harvested tree stem. The degree of bending stiffness as quantified by the static modulus of elasticity is one of the more important attributes associated with solid wood products, as reflected by its use in machine grading systems for classifying dimensional lumber products. This metric has traditionally been determined through destructive sampling procedures and, consequently, end-product quality of standing trees remains largely unknown until processed. However, as demonstrated in this study for jack pine trees, tree stiffness can be estimated via non-destructive means through its relationship with acoustic velocity and wood density and, hence, provides an alternative in-forest methodology for evaluating wood quality. Furthermore, the expansion of this primary acoustic-based relationship to include secondary relationships enabled the prediction of a suite of commercially-relevant fibre attributes that are associated with a broad array of potential end-products.

In summary, this study provided a parameterized suite of prediction models that could be of utility in forecasting end-product potential during pre-harvest inventories or informing post-harvest segregation and allocation decision-making for jack pine, contributed to solidifying the empirical foundation of the expanded acoustic-based inferential framework proposed for boreal conifers, and presented an alternative in-forest wood density determination method for potential deployment in acoustic-based sampling. Collectively, these results should be of utility in advancing the acoustic approach in value-based forest management decision-making.

Funding: Canadian Wood Fibre Centre (CWFC), Canadian Forest Service (CFS), Natural Resources Canada (NRCan).

Acknowledgments: The author expresses his appreciation to (1) Mike Laporte (Retired) of the CWFC, CFS, NRCan, and Gordon Brand of the Great Lakes Forestry Centre, CFS, NRCan for field and laboratory data acquisition and processing support, (2) Tong and Nelson Uy at FPInnovations Inc., for completing the SilviScan-3 analysis, (3) the CWFC, CFS, NRCan for fiscal support, and (4) anonymous reviewers for their insightful and constructive comments and suggestions.

Conflicts of Interest: The author declares no conflict of interest. The funder had no role in the design of the study, in the collection, analyses, or interpretation of data, in the writing of the manuscript, or in the decision to publish the results.

References

1. Natural Resources of Canada (NRCan). *The State of Canada's Forest*; NRCan: Ottawa, ON, Canada, 2018.
2. Emmett, B. Perspectives on sustainable development and sustainability in the Canadian forest sector. *For. Chron.* **2006**, *82*, 40–43. [CrossRef]
3. Malouin, C.; Larocque, G.R.; Doyle, M. Considerations of ecosystem services in ecological forest management. In *Ecological Forest Management Handbook*; Larocque, G.R., Ed.; CRC Press: Boca Raton, FL, USA, 2016; pp. 107–138.
4. Defo, M. SilviScan-3—A Revolutionary Technology for High-Speed Wood Microstructure and Properties Analysis. Midis de al Foresterie. UQAT. Available online: <http://chaireafd.uqat.ca/midiForesterie/pdf/20080422PresentationMauriceDefo.pdf> (accessed on 1 November 2018).
5. Murphy, G.; Cown, D. Stand, stem and log segregation based on wood properties: A review. *Scand. J. Res.* **2015**, *30*, 1–14. [CrossRef]
6. Ross, R.J. *Nondestructive Evaluation of Wood*; General Technical Report FPL-GTR-238; USDA, Forest Service, Forest Products Laboratory: Madison, WI, USA, 2015.
7. Wang, X. Acoustic measurements on trees and logs: A review and analysis. *Wood Sci. Technol.* **2013**, *47*, 965–975. [CrossRef]
8. Carter, P.; Briggs, D.; Ross, R.J.; Wang, X. Acoustic testing to enhance western forest values and meet customer wood quality needs. In *Productivity of Western Forests: A Forest Products Focus*; Harrington, C.A., Schoenholtz, S.H., Eds.; General Technical Report PNW-GTR-642; USDA, Forest Service, Pacific Northwest Research Station: Portland, OR, USA, 2005; pp. 121–129.

9. Wessels, C.B.; Malan, F.S.; Rypstra, T. A review of measurement methods used on standing trees for the prediction of some mechanical properties of timber. *Eur. J. Res.* **2011**, *130*, 881–893. [[CrossRef](#)]
10. Grabianowski, M.; Manley, B.; Walker, J.C.F. Acoustic measurements on standing trees, logs and green lumber. *Wood Sci. Technol.* **2006**, *40*, 205–216. [[CrossRef](#)]
11. Bucur, V. *Acoustics of Wood*; Springer: Berlin, Germany, 2006.
12. Wang, X.; Ross, R.J.; Carter, P. Acoustic evaluation of wood quality in standing trees. Part I. Acoustic wave behavior. *Wood Fiber Sci.* **2007**, *39*, 28–38.
13. Wang, X.; Carter, P. Acoustic assessment of wood quality in trees and logs. In *Nondestructive Evaluation of Wood*, 2nd ed.; Ross, R.J., Ed.; General Technical Report FPL-GTR-238; USDA, Forest Service, Forest Products Laboratory: Madison, WI, USA, 2015; pp. 87–102.
14. Newton, P.F. Acoustic-Based Non-Destructive Estimation of Wood Quality Attributes within Standing Red Pine Trees. *Forests* **2017**, *8*, 380. [[CrossRef](#)]
15. Hong, Z.; Fries, A.; Lundqvist, S.-O.; Gull, B.A.; Wu, H.X. Measuring stiffness using acoustic tool for Scots pine breeding selection. *Scand. J. Res.* **2015**, *30*, 1–10. [[CrossRef](#)]
16. National Lumber Grades Authority (NLGA). *Special Products Standard for Machine Graded Lumber*; NLGA: Surrey, BC, Canada, 2003.
17. National Lumber Grades Authority (NLGA). *Standard Grading Rules for Canadian Lumber*; NLGA: Surrey, BC, Canada, 2014.
18. Divós, F.; Tanaka, T. Relation between static and dynamic modulus of elasticity of wood. *Acta Silv. Lignaria Hung.* **2005**, *1*, 105–110.
19. Trofymow, J.A.; Koppenaal, R.S.; Filipescu, C.N. Late-rotation nitrogen fertilization of Douglas-fir: Growth response and fibre properties. *Can. J. For. Res.* **2017**, *47*, 134–138.
20. Desponts, M.; Perron, M.; Deblois, J. Rapid assessment of wood traits for large-scale breeding selection in *Picea mariana* [Mill.] B.S.P. *Ann. For. Sci.* **2017**, *74*, 53. [[CrossRef](#)]
21. Moore, J.R.; Dash, J.P.; Lee, J.R.; McKinley, R.B.; Dungey, H.S. Quantifying the influence of seedlot and stand density on growth, wood properties and the economics of growing radiata pine. *Forestry* **2017**, *91*, 327–340. [[CrossRef](#)]
22. Auty, D.; Achim, A. The relationship between standing tree acoustic assessment and timber quality in Scots pine and the practical implications for assessing timber quality from naturally regenerated stands. *Forestry* **2008**, *81*, 475–487. [[CrossRef](#)]
23. Wang, X.; Carter, P.; Ross, R.J.; Brashaw, B.K. Acoustic assessment of wood quality of raw materials: A path to increased profitability. *For. Prod. J.* **2007**, *57*, 6–14.
24. Legg, M.; Bradley, S. Measurement of stiffness of standing trees and felled logs using acoustics: A review. *J. Acoust. Soc. Am.* **2016**, *139*, 588–604. [[CrossRef](#)]
25. Zhang, S.Y.; Koubaa, A. *Softwoods of Eastern Canada: Their Silvics, Characteristics, Manufacturing and End-Uses*; Special Publication SP-526E; FPInnovations Inc.: Quebec City, QC, Canada, 2008.
26. Newton, P.F. Predictive Relationships between Acoustic Velocity and Wood Quality Attributes for Red Pine Logs. *For. Sci.* **2017**, *63*, 504–517. [[CrossRef](#)]
27. Newton, P.F. Acoustic velocity—wood fibre attribute relationships for jack pine logs and their potential utility. *Forests* **2018**, *9*, 749. [[CrossRef](#)]
28. Cave, I.D.; Walker, J.C.F. Stiffness of wood in fast-grown plantation softwoods: The influence of microfibril angle. *For. Prod. J.* **1994**, *44*, 43–48.
29. Evans, R.; Ilic, J. Rapid prediction of wood stiffness from microfibril angle and density. *For. Prod. J.* **2001**, *51*, 53–57.
30. Yang, J.L.; Evans, R. Prediction of MOE of eucalypt wood from microfibril angle and density. *Holz Roh Werkst.* **2003**, *61*, 449–452. [[CrossRef](#)]
31. Raymond, C.A.; Joe, B.; Evans, R.; Dickson, R.L. Relationship between timber grade, static and dynamic modulus of elasticity, and Silviscan properties for *Pinus radiata* in New South Wales. *N. Z. J. For. Sci.* **2007**, *37*, 186–196.
32. Newton, P.F. Development trends of black spruce fibre attributes in maturing plantations. *Int. J. For. Res.* **2016**, *2016*, 7895289.

33. Rinn, F.; Schweingruber, F.-H.; Schär, E. RESISTOGRAPH and X-Ray Density Charts of Wood. Comparative Evaluation of Drill Resistance Profiles and X-ray Density Charts of Different Wood Species. *Holzforschung* **1996**, *50*, 303–311. [[CrossRef](#)]
34. McKinnon, L.M.; Kayahara, G.J.; White, R.G. *Biological Framework for Commercial Thinning Even-Aged Single-Species Stands of Jack Pine, White Spruce, and Black Spruce in Ontario*; Report TR-046; Ontario Ministry of Natural Resources, Northeast Science and Information Section: South Porcupine, ON, Canada, 2006.
35. Carmean, W.H.; Hazenberg, G.; Niznowski, G.P. Polymorphic site index curves for jack pine in Northern Ontario. *For. Chron.* **2001**, *77*, 141–150. [[CrossRef](#)]
36. Rowe, J.S. *Forest Regions of Canada*; Publication No. 1300; Government of Canada, Department of Environment, Canadian Forestry Service: Ottawa, ON, Canada, 1972.
37. Evans, R. Rapid Measurement of the Transverse Dimensions of Tracheids in Radial Wood Sections from *Pinus radiata*. *Holzforschung* **1994**, *48*, 168–172. [[CrossRef](#)]
38. Evans, R.; Stuart, S.A.; Van Der Touw, J. Microfibril angle scanning of increment cores by X-ray diffractometry. *Appita J.* **1996**, *49*, 411–414.
39. Evans, R. Wood stiffness by X-ray diffractometry. In *Characterization of the Cellulosic Cell Wall*; Stokke, D.D., Groom, L.H., Eds.; Wiley: Hoboken, NJ, USA, 2006; pp. 138–146.
40. Neter, J.; Wasserman, W.; Kutner, M.H. *Applied Linear Statistical Models*, 3rd ed.; Irwin: Boston, MA, USA, 1990.
41. Raudenbush, S.W.; Bryk, A.S.; Cheong, Y.F.; Congdon, R.T., Jr. *HLM 7—Hierarchical Linear and Nonlinear Modeling*; Scientific Software International: Lincolnwood, IL, USA, 2011.
42. Reynolds, M.R., Jr. Estimating the error in model predictions. *For. Sci.* **1984**, *30*, 454–469.
43. Gribko, L.S.; Wiant, H.V., Jr. A SAS template program for the accuracy test. *Compiler* **1992**, *10*, 48–51.
44. Amishev, D.; Murphy, G.E. In-forest assessment of veneer grade Douglas-fir logs based on acoustic measurement of wood stiffness. *For. Prod. J.* **2008**, *58*, 42–47.
45. Lenz, P.; Bernier-Cardou, M.; Mackay, J.; Beaulieu, J. Can wood properties be predicted from the morphological traits of a tree? A canonical correlation study of plantation-grown white spruce. *Can. J. For. Res.* **2012**, *42*, 1518–1529. [[CrossRef](#)]
46. Kuprevicius, A.; Auty, D.; Achim, A.; Caspersen, J.P. Quantifying the influence of live crown ratio on the mechanical properties of clear wood. *Forests* **2013**, *86*, 361–369. [[CrossRef](#)]
47. Hayatgheibi, H.; Fries, A.; Kroon, J.; Wu, H.X. Genetic analysis of lodgepole pine (*Pinus contorta*) solid-wood quality traits. *Can. J. For. Res.* **2017**, *47*, 1303–1313. [[CrossRef](#)]
48. Chen, Z.-Q.; Karlsson, B.; Lundqvist, S.-O.; Gil, M.R.G.; Olsson, L.; Wu, H.X. Estimating solid wood properties using Pilodyn and acoustic velocity on standing trees of Norway spruce. *Ann. For. Sci.* **2015**, *72*, 499–508. [[CrossRef](#)]
49. Amateis, R.L.; Burkhart, H.E. Use of the fakopp treesonic acoustic device to estimate wood quality characteristics in loblolly pine trees planted at different densities. In Proceedings of the 17th Biennial Southern Silvicultural Research Conference; Holley, A., Gordon, H.A., Connor, K.F., Haywood, J.D., Eds.; General Technical Report SRS-203; USDA, Forest Service, Southern Research Station: Asheville, NC, USA, 2014; pp. 519–522.
50. Fischer, C.; Vestøl, G.I.; Øvrum, A.; Høibø, O.A. Pre-sorting of Norway spruce structural timber using acoustic measurements combined with site-, tree- and log characteristics. *Holz Roh Werkst.* **2015**, *73*, 819–828. [[CrossRef](#)]
51. Wang, X.; Ross, R.J.; McClellan, M.; Barbour, R.J.; Erickson, J.R.; Forsman, J.W.; McGinnis, G.D. *Strength and Stiffness Assessment of Standing Trees Using a Nondestructive Stress Wave Technique*; Research Paper FPL-RP-585; USDA, Forest Service, Forest Products Laboratory: Madison, WI, USA, 2000.
52. Nanami, N.; Nakamura, N.; Arima, T.; Okuma, M. Measuring the properties of standing trees with stress wave. Part III. Evaluation the properties of standing trees for some forest stands. *Mokuzai Gakkaishi* **1993**, *39*, 903–909.
53. Lachenbruch, B.; Johnson, G.R.; Downes, G.M.; Evans, R. Relationships of density, microfibril angle, and sound velocity with stiffness and strength in mature wood of Douglas-fir. *Can. J. For. Res.* **2010**, *40*, 55–64. [[CrossRef](#)]
54. Kang, H.; Booker, R.E. Variation of stress wave velocity with MC and temperature. *Wood Sci. Technol.* **2002**, *36*, 41–54. [[CrossRef](#)]

55. Chauhan, S.; Walker, J.; Chauhan, S. Variations in acoustic velocity and density with age, and their interrelationships in radiata pine. *For. Ecol. Manag.* **2006**, *229*, 388–394. [[CrossRef](#)]
56. Bérubé-Deschênes, A.; Franceschini, T.; Schneider, R. Factors Affecting Plantation Grown White Spruce (*Picea glauca*) Acoustic Velocity. *J. For.* **2016**, *114*, 629–637. [[CrossRef](#)]
57. Paradis, N.; Auty, D.; Carter, P.; Achim, A. Using a Standing-Tree Acoustic Tool to Identify Forest Stands for the Production of Mechanically-Graded Lumber. *Sensors* **2013**, *13*, 3394–3408. [[CrossRef](#)]
58. Leitch, M.; Miller, S. *Optimizing Wood Utilization Based on Whole Tree Inherent Property Maps*; Springer Science and Business Media LLC: Berlin/Heidelberg, Germany, 2017; pp. 3–17.
59. Newton, P.F. Quantifying the Effects of Wood Moisture and Temperature Variation on Time-of-Flight Acoustic Velocity Measures within Standing Red Pine and Jack Pine Trees. *Forests* **2018**, *9*, 527. [[CrossRef](#)]
60. Li, B.; Isik, F. Rapid assessment of wood density of live trees using the Resistograph for selection in tree improvement programs. *Can. J. For. Res.* **2003**, *33*, 2426–2435.
61. Downes, G.M.; Lausberg, M.; Potts, B.M.; Pilbeam, D.L.; Bird, M.; Bradshaw, B. Application of the IML Resistograph to the infield assessment of basic density in plantation eucalypts. *Aust. For.* **2018**, *81*, 1–9. [[CrossRef](#)]
62. Gao, S.; Wang, X.; Wiemann, M.C.; Brashaw, B.K.; Ross, R.J.; Wang, L. A critical analysis of methods for rapid and non-destructive determination of wood density in standing trees. *Ann. For. Sci.* **2017**, *74*, 27. [[CrossRef](#)]
63. Wu, S.-J.; Xu, J.-M.; Li, G.-Y.; Risto, V.; Lu, Z.-H.; Li, B.-Q.; Wang, W. Use of the pilodyn for assessing wood properties in standing trees of Eucalyptus clones. *J. For. Res.* **2010**, *21*, 68–72. [[CrossRef](#)]
64. Defo, M.; Dalpke, B.; Sherson, G.; Xu, Q.; Qin, M.; Ni, Y. Predictions of wood density and module of elasticity of balsam fir (*Abies balsamea*) and black spruce (*Picea mariana*) from near infrared spectral analyses. *Can. J. For. Res.* **2011**, *41*, 352–358.
65. Green, D.W.; Winandy, J.E.; Kretschmann, D.E. *Wood as an Engineering Material*; General Technical Report FPL-GTR-113; USDA, Forest Service; Forest Products Laboratory: Madison, WI, USA, 1999.
66. Bodig, J.; Goodman, J.R. Prediction of elastic parameters of wood. *Wood Sci.* **1973**, *5*, 249–264.
67. Proto, A.R.; Macri, G.; Bernardini, V.; Russo, D.; Zimbalatti, G. Acoustic evaluation of wood quality with a non-destructive method in standing trees: A first survey in Italy. *iForest* **2017**, *10*, 700–706. [[CrossRef](#)]
68. Russo, D.; Marziliano, P.A.; Macri, G.; Proto, A.R.; Zimbalatti, G.; Lombardi, F. Does Thinning Intensity Affect Wood Quality? An Analysis of Calabrian Pine in Southern Italy Using a Non-Destructive Acoustic Method. *Forests* **2019**, *10*, 303. [[CrossRef](#)]
69. Murphy, G.E.; Moore, J.R. SEGMOD—A techno-economic model for evaluating the impact of segregation based on internal wood properties. *Ann. For. Sci.* **2018**, *75*, 73. [[CrossRef](#)]
70. Gao, S.; Wang, X.; Wang, L.; Allison, R.B. Effect of temperature on acoustic evaluation of stand trees and logs: Part 2: Field investigation. *Wood Fibre Sci.* **2013**, *45*, 15–25.

